International Geology Review

ISSN: (Print) (Online) Journal homepage: https://www.tandfonline.com/loi/tigr20

Neoproterozoic pre-collisional events recorded in the Sergipano belt, Southern Borborema Province, West Gondwana

Luiz Henrique Passos, Reinhardt A. Fuck, Farid Chemale Junior, Cristine Lenz, Carla Cristine Porcher, Viter Magalhães Pinto & Lauro Cézar M. de Lira Santos

To cite this article: Luiz Henrique Passos, Reinhardt A. Fuck, Farid Chemale Junior, Cristine Lenz, Carla Cristine Porcher, Viter Magalhães Pinto & Lauro Cézar M. de Lira Santos (2023) Neoproterozoic pre-collisional events recorded in the Sergipano belt, Southern Borborema Province, West Gondwana, International Geology Review, 65:4, 527-545, DOI: 10.1080/00206814.2022.2054029

To link to this article: https://doi.org/10.1080/00206814.2022.2054029

INTERNATIONAL GEOLOGY REVIEW
2023, VOL. 65, NO. 4, 527–545
https://doi.org/10.1080/00206814.2022.2054029

Taylor & Francis
Taylor & Francis Group

Neoproterozoic pre-collisional events recorded in the Sergipano belt, Southern Borborema Province, West Gondwana

Luiz Henrique Passos[a], Reinhardt A. Fuck[a], Farid Chemale Junior[b], Cristine Lenz[c], Carla Cristine Porcher[d], Viter Magalhães Pinto[e] and Lauro Cézar M. de Lira Santos[f]

[a]Instituto de Geociências, Universidade de Brasília, Campus Universitário Darcy Ribeiro, Brasília, Brazil; [b]Programa de Pós-Graduação em Geologia, Universidade do Vale do Rio dos Sinos, São Leopoldo, Brazil; [c]Departamento de Geologia, Universidade Federal de Sergipe, Campus São Cristóvão, São Cristóvão, Brazil; [d]Instituto de Geociências, Universidade Federal do Rio Grande do Sul, Porto Alegre, Brazil; [e]Centro de Engenharia, Engenharia Geológica, Universidade Federal de Pelotas, Pelotas, Brazil; [f]Departamento de Geologia, Universidade Federal de Pernambuco, Recife, Brazil

ABSTRACT

The Canindé Domain is crucial for understanding the pre-collisional events in Sergipano Belt, Borborema Province, especially during the Late Stenian/Early Tonian (740–680 Ma). We present thermobarometric, geochronology, and isotopic studies of the metavolcanosedimentary rocks of the Novo Gosto unit. The calculated metamorphic conditions resulted in a range of T: 600–740°C and P: 3.5–10.0 kbar for non-mylonitic amphibolites and values of T: 636–808°C and P: 7.0–12.0 kbar for mylonites, both of amphibolite facies. The minimum metamorphic conditions imprint in these rocks are T: 390°C and P: 2.5 kbar, indicating retrometamorphism in greenschist facies. The probable age of the peak metamorphic event was obtained in zircon rims from a quartzite at 692 ± 8.5 Ma. U-Pb detrital zircon and Nd model ages of the metasedimentary rocks point out Early Tonian as primary source rocks. Subordinate contributions of Mesoproterozoic, Paleoproterozoic, and Neoarchean sources were also recognized. These primary sources are related to Cariris Velhos event rocks, whereas the subordinate sources are from the Pernambuco-Alagoas superterrane. Early Tonian and Late Stenian ages were recognized for the first time in the Canindé Domain, with U-Pb zircon ages of 1005 ± 3 and 989 ± 6 Ma in amphibolites and mylonitized granites, mostly outcropping at the southwestern limit of the area. New ages were also obtained in the Novo Gosto surrounding intrusions: Canindé Layered Gabbroic Intrusion (~718 Ma), Garrote (~715 Ma) and Curralinho/Boa Esperança (~708 Ma) metagranites, and Gentileza metavolcanic rock (~700), which integrate the early pre-collisional magmatism of the Sergipano Belt (~740-680 Ma). Finally, U-Pb zircon ages were obtained in the Poço Redondo Domain, potential source area of the Novo Gosto metasedimentary rocks, resulting in ages of 957 ± 11 and 988 ± 15 Ma. The new data bring perspective to future correlations with adjacent belts and the understanding of the structuration of West Gondwana during the Brasiliano-Pan-African Orogeny.

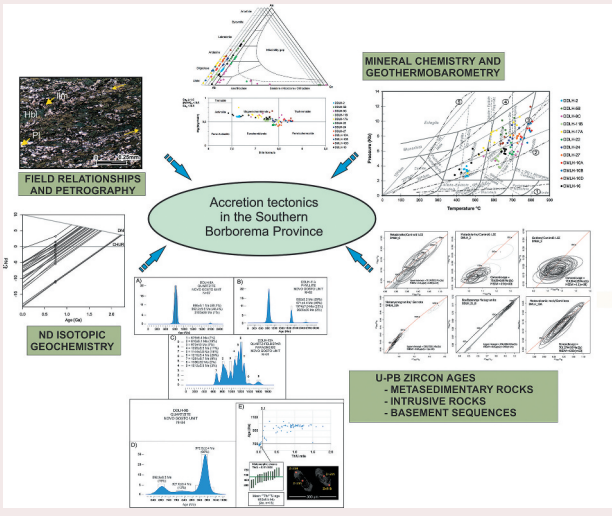

ARTICLE HISTORY
Received 18 November 2021
Accepted 12 March 2022

KEYWORDS
Sergipano belt; pre-collisional rocks; metamorphic conditions; Nd isotopes; U-Pb ages

CONTACT Luiz Henrique Passos lhpassos.geologo@gmail.com Instituto de Geociências, Universidade de Brasília, Campus Universitário Darcy Ribeiro, Brasília DF, Brazil

Supplemental data for this article can be accessed here

1. Introduction

The study of Neoproterozoic orogenic belts is of fundamental importance to understand the evolution of lithospheric pieces that were once part of the Gondwana continent. In the Borborema Province (NE Brazil), several accretionary and collisional events have been documented along these fragments, being mostly attributed to the Brasiliano-Pan African Orogeny (e.g. Brito Neves *et al*. 2014; Caxito *et al*. 2020; Santos *et al*. 2021).

This province is mostly composed of Paleoproterozoic basement domains that were overlain and/or intruded by Neoproterozoic metamorphic and magmatic rocks, also including local Archean nuclei (Brito Neves *et al*. 2001). Its orogenic record has been intensively debated, pointing out to accretionary, collisional, and intracontinental deformation styles (e.g. Kozuch 2003; Oliveira *et al*. 2010; Amaral *et al*. 2012; Caxito *et al*. 2014, 2021; Lima *et al*. 2015, 2017, 2018; Santos *et al*. 2015; Lages and Dantas 2016; Padilha *et al*. 2016). Evidence for oceanic crust consumption and collisional tectonics that took place during the assembly of Western Gondwana in the province is marked by magmatic arc associations, disrupted ophiolite preserved remnants and high-grade metamorphic rock sequences (Santos and Caxito 2021).

The Sergipano Belt occupies part of the southern Borborema Province and has received major attention due to the wide exposition of magmatic and metavolcanosedimentary rocks that were generated via distinct stages of the Wilson Cycle during the Neoproterozoic (Oliveira *et al*. 2010). In addition, a substantial amount of published geochemical and isotopic data has provided clues for a record of the orogenic history of the region, including the primitive arc-related rocks aged at ca. 740 Ma (Passos *et al*. 2021), bringing a new perspective for early stages of the Brasiliano Orogeny.

In this research, we studied early Tonian rocks within the metavolcanosedimentary Canindé domain of the Sergipano Fold Belt, presenting new petrographic data and exploring the P-T constraints in metavolcanic rocks locally known as Novo Gosto Unit. We also present new U-Pb zircon ages and Sm-Nd data, providing essential information about the source area, metamorphic peak and crystallization ages of related intrusive rocks, adding a contribution about the early development of accretionary phases of the Southern Borborema Province and correlations along Western Gondwana.

2. Geological setting

The Sergipano Belt is an E-SE to W-NW trending fold and thrust belt (Figure 1A,B), cropping out between the São Francisco-Congo Craton and the Pernambuco-Alagoas superterrane of the Borborema Province (Oliveira *et al*. 2010; Brito Neves and Silva Filho 2019). It was formed due to collisional episodes between the cratonic area and smaller blocks that now form the basement of the Borborema Province (Brito Neves *et al*. 1977; Del-rey Silva 1995). The belt stratigraphy comprises five domains, from north to south, named as Canindé, Poço Redondo-Marancó, Macururé, Vaza Barris and Estância, which are bounded by late Neoproterozoic to Cambrian regional-scale shear zones (Davison and Santos 1989; Silva Filho 1998) (Figure 1B).

The Canindé domain occupies the northernmost part of the Sergipano Belt (Figure 1B,C) and it is limited with the Poço Redondo-Marancó domain by the Mulungu-Alto Bonito Shear Zone (Figure 1B). It is composed of (i) the Canindé Complex rocks (metavolcanic-sedimentary rocks of the Novo Gosto unit and bimodal hypabyssal rocks of the Gentileza unit), (ii) Canindé layered gabbroic intrusion, and (iii) pre-, syn- and post-collisional late Neoproterozoic intrusive granitic suites. The Novo Gosto unit consists of amphibolites, feldspathic quartzites, metarythmites, metapelites, marbles, and calc-silicate rocks. So far, the available geochronological data of the Novo Gosto unit rocks are restricted to a marble sample aged at 963 ± 20 Ma ($^{207}Pb/^{206}Pb$) and interpreted by Nascimento (2005) as the maximum depositional age of the sedimentary pile, whilst Oliveira *et al*. (2015) obtained a maximum deposition age of approximately 650 Ma (U-Pb SHRIMP zircon) in a metagraywacke sample. Lastly, Passos *et al*. (2021) reported a zircon U-Pb age (LA-ICPMS) of 743 ± 3 Ma for a metavolcanic rock sample, interpreted as the crystallization age of the rock and the single magmatic age obtained of the metavolcanosedimentary sequence.

3. Methodology

3.1 Mineral chemistry and geothermobarometry

Mineral chemistry of the amphibolites was carried out in two laboratories: I–In the Laboratory of Electron Microprobe (LASON) of the Universidade de Brasília (DMLH-10A, DMLH-10B, DMLH-10C, DMLH-16), with a JEOL JXA-8230 probe with five WDS spectrometers and an EDS. The analyzer crystals available in the probe (TAPJ, LIF, LIFH, PETJ, PETH, LDE1, and LDE2) allow the measurement of all chemical elements with an atomic number larger than 4. The probe was calibrated with an acceleration voltage of 15 kV and a current of 10 nA. II – The remaining samples were analyzed at the Electron Microprobe Laboratory of the Institute of Geosciences of the Universidade Federal do Rio Grande do Sul (CPGq-

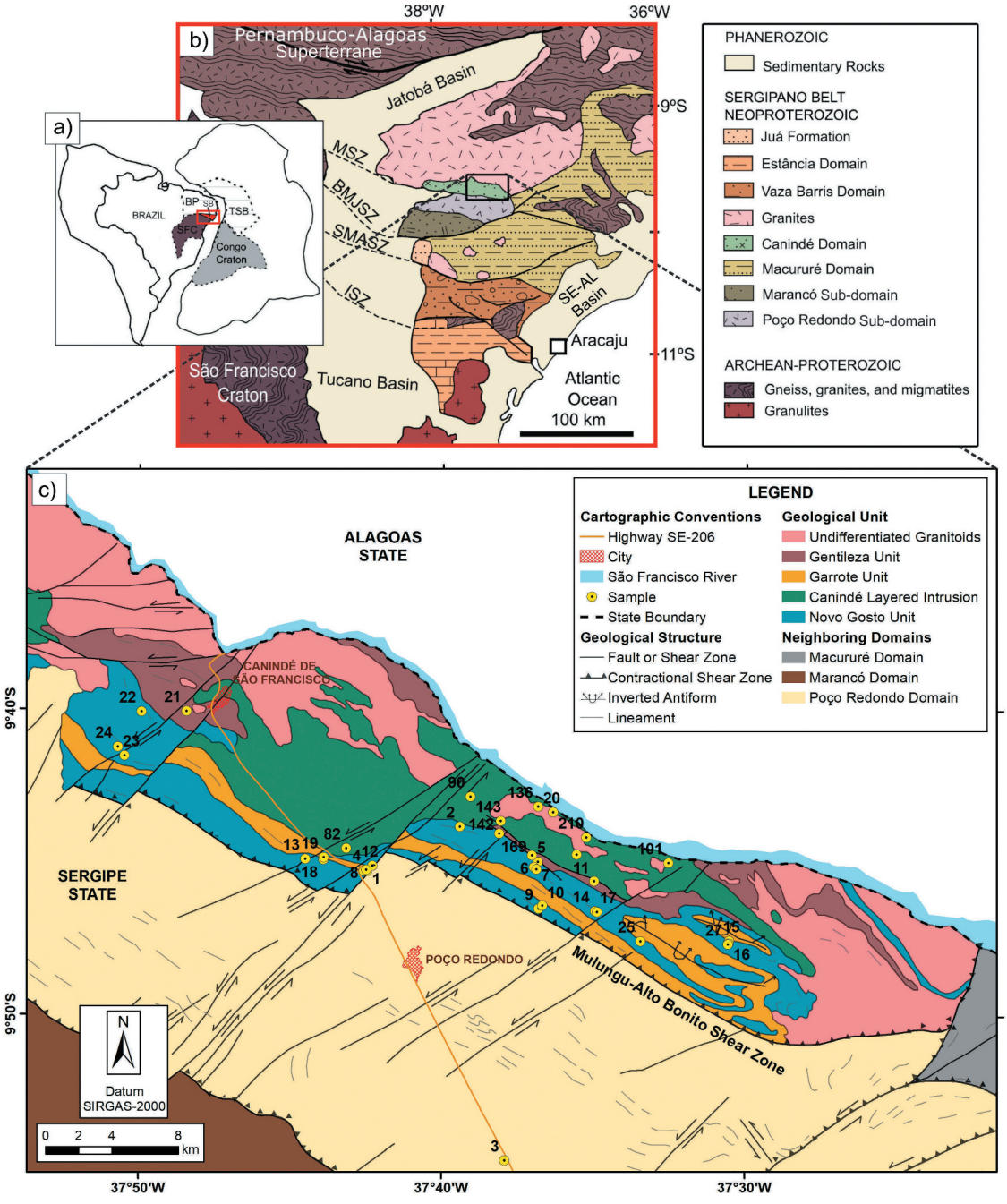

Figure 1. (A) Paleogeographic reconstruction showing the Neoproterozoic connection between the Borborema Province (BP, NE Brazil) and the Trans-Saharan belt (TSB, NW Africa). SB (Sergipano Belt), SFC (São Francisco craton). (B) Geological map of the Sergipano Belt. MSZ (Macururé Shear Zone), BMJSZ (Belo Monte-Jeremoabo Shear Zone), SMASZ (São Miguel do Aleixo Shear Zone), ISZ (Itaporanga Shear Zone). (C) Geological map of the central Canindé domain with the location of studied samples (Supp. Table 1). Modified by Passos *et al*. (2021) from D'el-rey Silva (1995) and Santos *et al*. (1998).

IGEO-UFRGS). The laboratory is equipped with a CAMECA SXFive micro-analyzer, which performed the analyses with operation conditions of 15 keV accelerating voltage and 20 nA beam current.

In both laboratories, crystals of feldspar, amphibole, titanite, chlorite, and opaque minerals were analyzed, and the contents of SiO_2, TiO_2, Al_2O_3, FeO, MnO, MgO, CaO, K_2O, Na_2O, V_2O_3, NiO, Cr_2O_3, and OH were determined. The results were processed in the WinAmptb (Yavuz and Döner 2017), WinCcac (Yavuz *et al*. 2015), and Microsoft Excel software, and were then plotted on classification diagrams for the analyzed minerals.

The amphibole was chosen to calculate the P-T conditions and the data were plotted in the WinAmptb software (Yavuz and Döner 2017) which is

built to perform thermobarometry calculations. The calculation methods are those adopted by Ernst and Liu (1998) (Al-in-amp barometer – kbars; amp-only thermometer – °C) and the results were plotted on a P-T diagram with the metamorphic facies fields.

3.2 Whole-rock Nd isotope analyses

Fifteen samples of metasedimentary rocks (Supp. Table 1) were selected and pulverized for Sm-Nd analyses at the Geochronology Laboratory of Universidade de Brasília and followed the methodology described in Gioia and Pimentel (2000). About 50 mg of whole-rock powder was mixed with ^{149}Sm-^{150}Nd spike solution and dissolved in Savillex capsules. The extractions of Sm and Nd were carried out on Teflon columns containing LN-Spec resin (HDEHP – Di-(2-Ethylhexyl) phosphoric acid supported by polytetrafluorethylene powder). The Sm and Nd fractions were placed into double rhenium filament arrays and the isotopic measurements were done in a Finnigan TRITON multi-collector mass spectrometer in static mode. The uncertainties for Sm/Nd and $^{143}Nd/^{144}Nd$ are better than ±0.5% (2σ) and ±0.005% (2σ), respectively, based on repeated analyses of the BHVO-2 and BCR-1 rock standards. The $^{143}Nd/^{144}Nd$ ratios are normalized to $^{146}Nd/^{144}Nd$ of 0.7219 and the decay constant (λ) used was 6.54×10^{-12}. Data were processed in the GCDKit 5.0 package used as a complement to the R 3.5.3 software (Janoušek *et al*. 2019). $\varepsilon_{Nd}(t)$ values were calculated using the U-Pb ages defined from zircon grains or estimated ages based on the regional and current results from nearby samples. 1-stage and 2-stage Nd model ages are calculated after Goldstein *et al*. (1984).

3.3 U-Pb zircon geochronology

Fifteen samples were collected, including rocks representative of the units considered as older and rocks of undetermined origin exposed within the limits of the Canindé domain (Supp. Tables 1, 2). The samples were crushed and milled using a jaw crusher and swing mill. Heavy minerals were separated by conventional procedures using a magnetic separator and heavy liquids. Zircon was concentrated by handpicking, mounted in epoxy resin and polished. The U-Pb isotopic analyses were performed using the Laser Ablation Multi-Collector Inductively Coupled Plasma Mass Spectrometry (LA-MC-ICP-MS) at Universidade de Brasília (UnB), Laser Ablation Sector Field Inductively Coupled Plasma Mass Spectrometry (LA-SF-ICP-MS) at Universidade Federal de Ouro Preto (UFOP), and Sensitive High-Resolution Ion Microprobe (SHRIMP) at the Australian National University (ANU).

Isotopic data obtained by the LA-MC-ICP-MS were acquired using static mode with 25 μm spot size. Data acquisition occurred in 40 cycles of 1.048 s of integration time, and the 202, 204, 206, 207, 208, 232, and 238 masses were collected simultaneously, 202, 204, 206, 207, and 208 measured with multiplier ion counting and 232 and 238 with Faraday cups. Laser-induced elemental fractional and instrumental mass discrimination were corrected using the GJ-1 reference zircon (Jackson *et al*. 2004). During the analytical sessions, the zircon standard 91,500 (Wiedenbeck *et al*., 1995; 2004)[1] was also analyzed as an external standard. U-Th-Pb data reduction was calculated in an Excel spreadsheet (Chemale *et al*. 2012) and details of instrumental operating conditions followed Bühn *et al*. (2009).

LA-SF-ICP-MS data were acquired in peak jumping mode during 20s background measurement followed by 20s sample ablation with a spot size of 20 μm, laser energy of 15%, shot frequency of 10 Hz, and shutter delay of 15s. To evaluate the accuracy and precision of the laser-ablation results, we analyzed BB-1 zircon (562.58 ± 0.26 Ma; Santos *et al*. 2017), Plešovice zircon (337 ± 1 Ma; Sláma *et al*. 2008), GJ-1 zircon (608.5 ± 1.5 Ma; Jackson *et al*. 2004). The obtained ages were concordant with the experimental errors, where the obtained concordant ages were 562.64 ± 1.20 Ma (n = 15, 2s.) for BB-1, 337.30 ± 0.56 Ma (n = 25, 2s.) for Pleisovice, and 601.44 ± 4.72 Ma (n = 60, 95% conf.) for GJ-1. For both methods, raw data were corrected for background signal, and laser-induced elemental fractionation and instrumental mass discrimination were corrected with reference to zircon GJ-1 (Jackson *et al*. 2004). Common Pb correction was based on the Pb composition model (Stacey and Kramer 1975). Data were corrected and reduced using software Glitter (Van Achterbergh *et al*. 2001).

The Poço Redondo domain samples were analyzed by the U-Pb SHRIMP (Sensitive High-Resolution Ion Microprobe) zircon geochronology, at the Research School of Earth Sciences, Australian National University using SHRIMP II equipment. Handpicked zircon grains were mounted in epoxy discs along with zircon standards, ground and polished, microphotographed in transmitted and reflected light, and their internal zoning imaged by cathodoluminescence (CL) using a scanning electron microscope. The mounts were then cleaned and gold-coated in preparation for SHRIMP analysis. Analytical methods and data

[1] Wiedenbeck et al., 1995, 2004 is cited in the references

treatment can be found elsewhere (Compston *et al*. 1984; Williams 1998). Zircon grains were analysed with a 2–3nA, 10kV primary O_2^- beam focused to a ~ 25 to ~20 μm diameter spot. At mass resolution ~5500 the Pb, Th, and U isotopes were resolved from all significant interferences. Reduction of raw data and age calculation were carried out using Squid 2.02 and Isoplot-Ex (Ludwig 2003). U and Th concentrations were determined relative to those measured in the RSES standard SL13.

The U-Pb Concordia diagrams and histograms were processed using IsoplotR 2.4 (Vermeesch 2018). We used $^{206}Pb/^{238}U$ – $^{207}Pb/^{206}Pb$ age cutoff of 1000 Ma for the detrital zircon grains with a 100 ± 10% concordance. The U-Pb zircon data are presented in the supplementary material (Supp. Material 1).

4. Results

4.1 Field relationships and petrography

The Novo Gosto unit metavolcanic rocks are mostly amphibolites and are found as isolated bodies or interleaved with metasedimentary rocks (Figures 2A, B). These rocks occur preferentially and more continuously in the southernmost part of the Canindé domain. They are fine-grained rocks, with mostly greenish black to lighter greenish colours with moderate weathering (Figure 2F). Due to deformation and metamorphism, igneous (protolith) textural evidence is not commonly observed in mesoscopic scale. However, punctual porphyroclasts of ancient feldspar phenocrysts can be identified, in addition to sinuous contacts and reaction rims with the neighbouring metasedimentary rocks, which we suggest that reflect intrusive contacts.

Depending on the distance from the shear zones, the rocks show variable deformation degrees. For instance, in the vicinity of these structures, amphibolites show well-developed mylonitic foliation (Figure 2C). In contrast, away from these zones the rocks tend to have poor-developed to incipient foliation planes and lack of evident deformation markers. In the southern region of the domain, contacts with the surrounding rocks are dominantly tectonic due to the shear zones influence (Figure 2F). Xenoliths of the Novo Gosto unit are also widespread within the Garrote granite and in the Canindé layered gabbroic intrusion (Figure 2E).

In microscale, the amphibolites are fine to very fine-grained (Figure 3). They show mm- to cm mylonitic foliation or deformed magmatic bands, alternating amphibole-rich and plagioclase-rich bands, but slightly deformed samples are present. The dominant texture is nematoblastic, defined by the preferred orientation of elongated amphibole crystals (Figures 3A,B,C,E) and plagioclase-dominated aggregates. These rocks mineralogy include hornblende (30–83%), plagioclase (7–45%) and opaque minerals (trace-15%). Other phases include titanite (trace-14%), epidote (trace-8%), chlorite (up to 13%), sericite (trace), quartz (up to 3%), K-feldspar (trace), carbonate (trace-2%), apatite (trace) and zircon (trace) (Supp. Table 3).

Amphibole occurs with brownish-green, green, and bluish-green colours, anhedral to subhedral crystalline habits, with straight to irregular contacts with the adjacent phases. The deformed members present several markers of ductile deformation (Figure 3D), including the formation of small sub-grains at the edges of larger crystals with some edge migration, SC structures (Figure 3D), *augen*-like fabrics with ilmenite crystals developing pressure shadows, undulose extinction, crystals with fish-like structure. When aligned fabric is not evident, polygonal granoblastic texture predominate. Some crystals contain inclusions of opaque minerals, plagioclase, quartz, apatite, and zircon forming poikiloblastic textures. In some samples, amphibole occurs with bluish-green edges, possibly related to compositional changes due to retrometamorphism. Amphibole minerals are also replaced by chlorite and epidote, which are interpreted as the main secondary phases in these rocks.

Quartz and K-feldspar crystals may be present but are not common. They are generally associated with plagioclase in felsic bands following the major foliation orientations. They occur as anhedral to euhedral crystals, with irregular to straight contacts, exhibiting well-developed polygonal texture. Epidote can also fill fractures, probably associated with hydrothermal remobilization (Figure 3F). In some samples, reddish chlorite was identified as an alteration of amphibole, most frequently occurring along fractures possibly related to hydrothermal alteration either. Carbonate is found in mylonitic amphibolites forming discordant venules with respect to the rock foliation. Carbonate concentrations in oval fabrics might be present, possibly representing old calcium plagioclase microlites.

4.2 Mineral chemistry and geothermobarometry

Mineral chemistry was acquired in phases that we interpreted as the record of the metamorphic assemblage. Chemistry was used, at first, to determine the classification and structural formulas in feldspar (n = 109), amphibole (n = 99), opaque minerals (n = 47), chlorite (n = 8) and titanite (n = 14) (supplementary materials SP2, 3, 4, 5, 6).

Data for plagioclase (Supp. Material 2) show albite, oligoclase, and andesine (Figure 4A) and rarely labradorite field on the An-Ab-Or diagram of Deer *et al*.

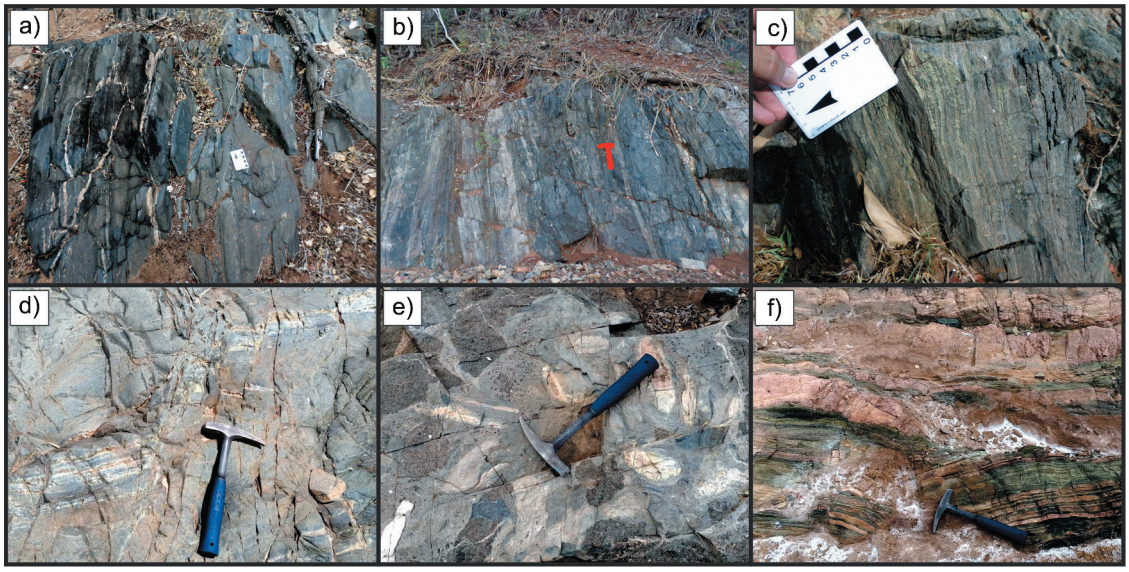

Figure 2. Rocks from the Canindé domain of the Sergipano belt. (A) Amphibolite with incipient foliation, far from the Mulungu-Alto Bonito shear zone; (B) Amphibolite interleaved with metasedimentary rock; (C) Mylonitic amphibolite in the Mulungu-Alto Bonito shear zone; (D) Amphibolite with sinistral NE fault, related to late ruptile deformation that affected the Canindé domain; (E) Xenoliths of the Novo Gosto unit in the Canindé layered gabbroic intrusion; (F) Epidotized amphibolites from the Novo Gosto unit in tectonic contact with the Garrote granite in a shear zone.

(1992). When present, K-feldspar is a minor phase, whose dominant chemical composition points to compositional variation of calcium-rich plagioclase crystals for more sodium-rich crystals can be related

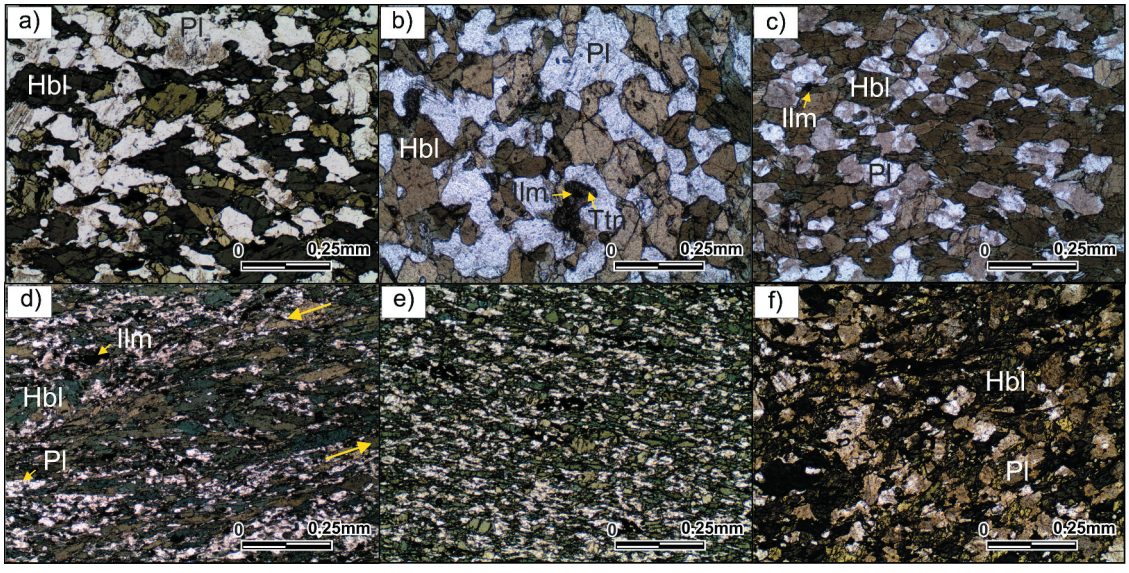

Figure 3. Mineralogical and textural aspects of the amphibolites from the Novo Gosto unit. Samples (A) (DDLH-27), (B) (DMLH-16) and (C) are amphibolites with nematoblastic to polygonal texture, less foliated and coarser-grained ones (V-11); (D) Mylonitic amphibolite with S-C foliation bands (DMLH-10A); (E) Foliated and very fine-grained amphibolite (DDLH-11B); (F) Foliated amphibolite with altered feldspar crystals (DDLH-9C).

anorthoclase and orthoclase (Figure 4A). The to the variation of P-T conditions in the rock.

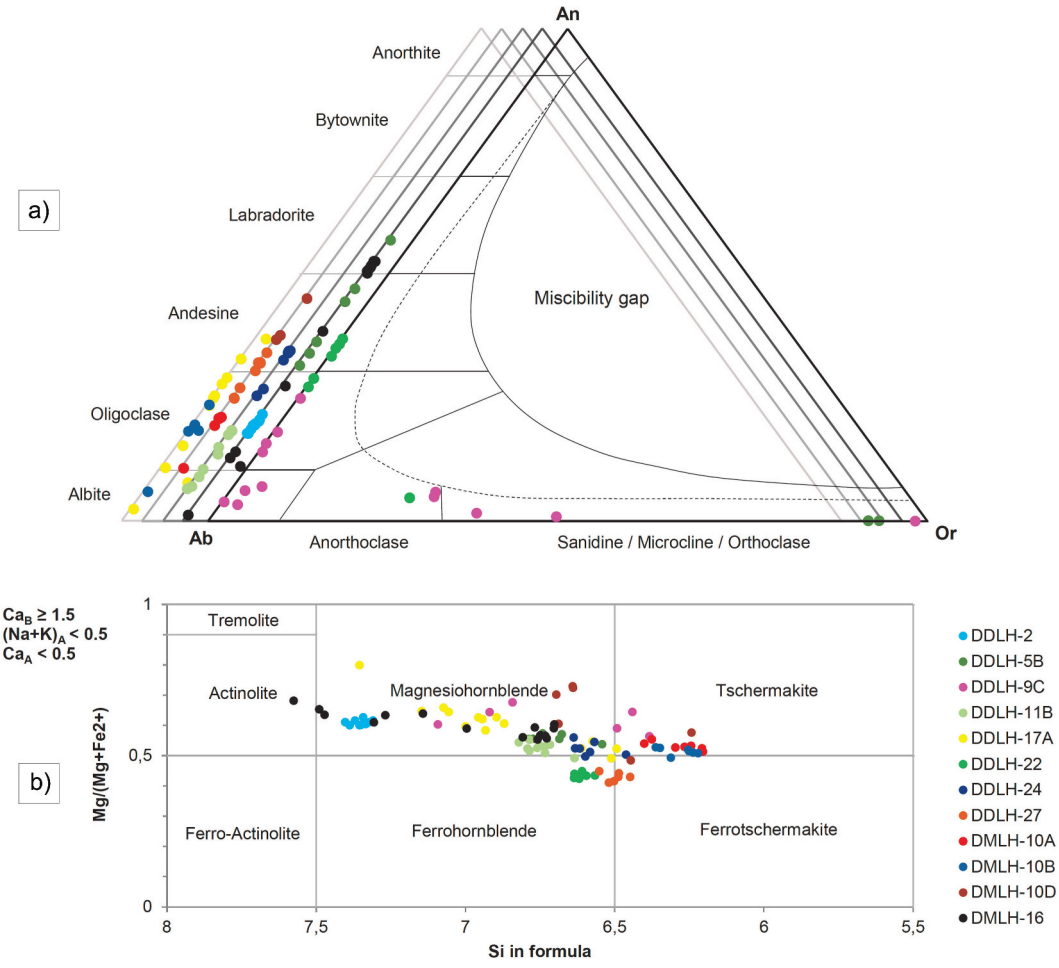

Figure 4. (A) An-Ab-Or feldspar ternary diagram with the feldspar composition of the samples from the Novo Gosto Unit plotted (Deer *et al*. 1992); (B) Amphibole classification diagram of analyzed amphiboles (Leake *et al*. (1997); Mg, Fe2+, Si are per formula. Samples DMLH-10A, 10B e 10D are mylonitic.

In general, the analyzed amphibole crystals were classified as calcium amphiboles. The analyses (Supp. Material 3) plotted on the Si × Mg/(Mg+Fe^{2+}) diagram of Leake *et al*. (1997) form an alignment starting from the actinolite field and passing through the magnesiohornblende field, partially corresponding to tschermakite, ferrotschermakite, and ferrohornblende (Figure 4B). In some samples, the amphibole crystals show zonation, switching to actinolite at the edges, which can be an effect of the retrometamorphism that affected the rock.

Analyses of titanite crystals (Supp. Material 4) in the Fe versus Al cations per formula unit diagram (Ling *et al*. 2015) plot mostly in the metamorphic origin field (Figure 5A). The chlorite crystals (Supp. Material 5) were plotted in the Al + vacancy – Mg – Fe ternary diagram (Zane and Weiss 1998) and mostly plot in the field of trioctahedral chlorites, with variations between the fields of chamosite and clinochlore (Figure 5B). Only one sample plotted in the field of dioctahedral aluminous chlorites.

Analyses of opaque mineral crystals (Supp. Material 6), plotted in the TiO_2 – FeO – Fe_2O_3 ternary diagram (Cerny *et al*. 2016; after Piper 1987; Cornell and Schwertmann 2003) show that ilmenite is the dominant phase in the amphibolites (Figure 5C). It was generated by the breaking of ilmenite, possibly due to the influence of hydrothermal fluids in the shear zones.

The P and T values were estimated using the method described in section 4. A wide range of P-T conditions were obtained, with a variation in P between 2.5 and 12.0 kbar and in T between 390°C and 808°C (the complete data can be found in Supp. Table 4 and summarized in Supp. Table 5). Pressure conditions vary mostly between 4.0 and 10.0. Temperature conditions vary mostly between 550°C and 750°C.

Mylonitic amphibolites show the highest P and T conditions, which is consistent with the identified textures in the microscale. In the non-mylonitized

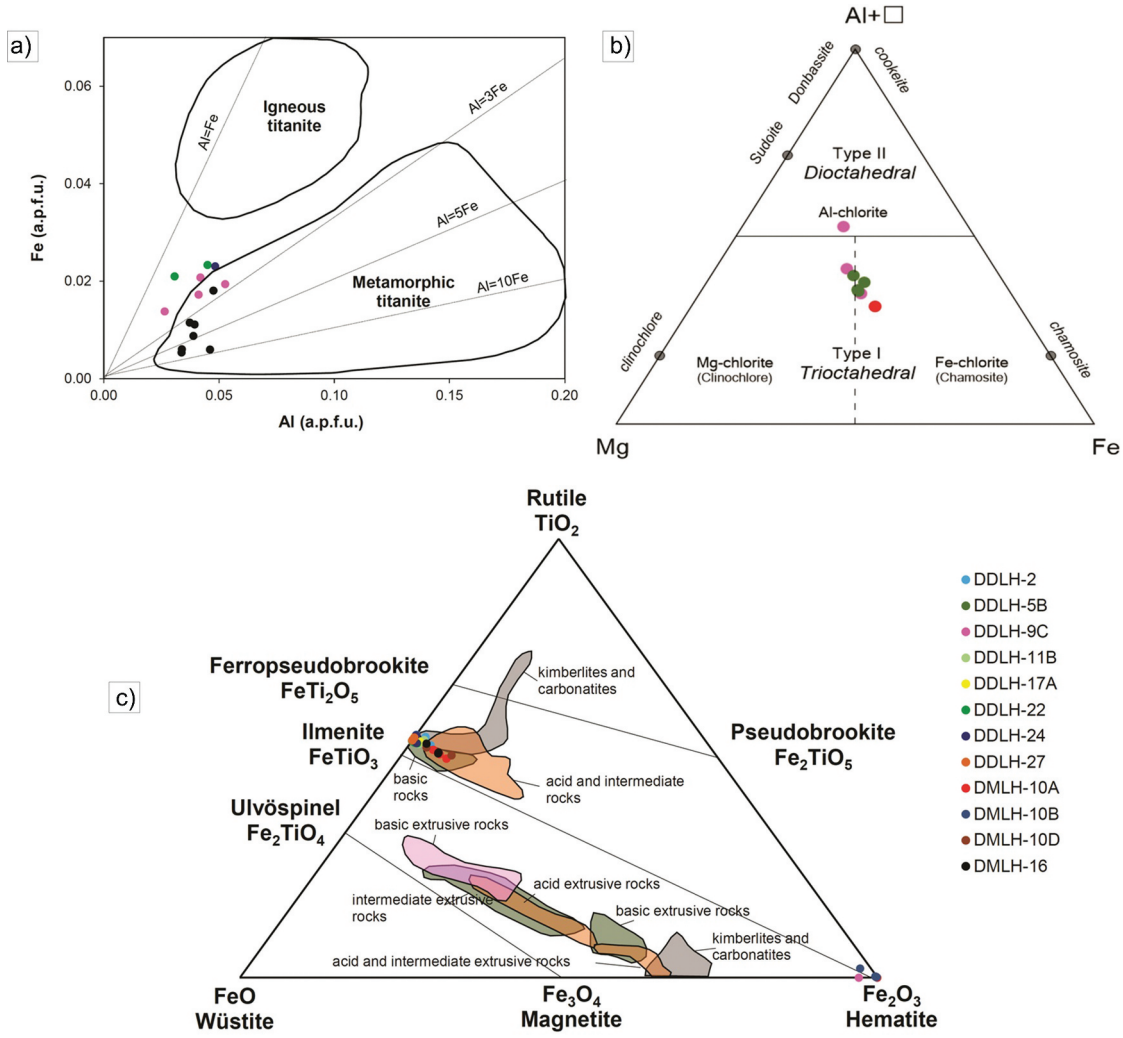

Figure 5. (A) A plot of the analysis of samples from the Novo Gosto Unit in the Fe versus Al cations per formula unit (Ling *et al*. 2015 after Aleinikoff *et al*. 2002; Rasmussen *et al*. 2013); (B) Chlorite analyses plotted in the Al+□ – Mg – Fe ternary diagram (Zane and Weiss 1998); (C) Opaque minerals analysis plotted in the composition diagram of titanomagnetite and titanohematite in various types of igneous rocks (Cerny *et al*. 2016; after Piper 1987; Cornell and Schwertmann 2003). Samples DMLH-10A, 10B e 10D are mylonitic.

samples, P-T values achieve a maximum T of 808°C and P of 12 kbars, which is similar to those from the mylonitic samples.

4.3 U-Pb zircon ages

U-Pb ages (Supp. Table 2, Supp. Material 1) from zircon grains are from four metasedimentary samples from the Novo Gosto unit. Intrusive rocks were investigated, with three samples dated in the Canindé Gabbroic Layered Intrusion and one sample each in the Garrote metagranite, Curralinho/Boa Esperança metagranite, and Gentileza amphibolite. Finally, four samples of the basement (Poço Redondo domain) were also analyzed, of which two are exposed in the Poço Redondo domain and two are exposed as tectonic slices in the Novo Gosto unit.

4.3.1 Novo gosto unit detrital zircon grains

Detrital zircon grains from metasedimentary rocks of the Novo Gosto unit were investigated to establish their maximum depositional age and provenance (Supp. Table 2, Supp. Material 1).

Sixty-seven zircon analyses of quartzite sample DDLH-9A resulted in three peaks of detrital zircon grains at 895 ± 5.1 Ma (50.1%), 962.2 ± 5.6 Ma (48.4%), 2100 ± 36 Ma (1%) (Figure 6A). The age at

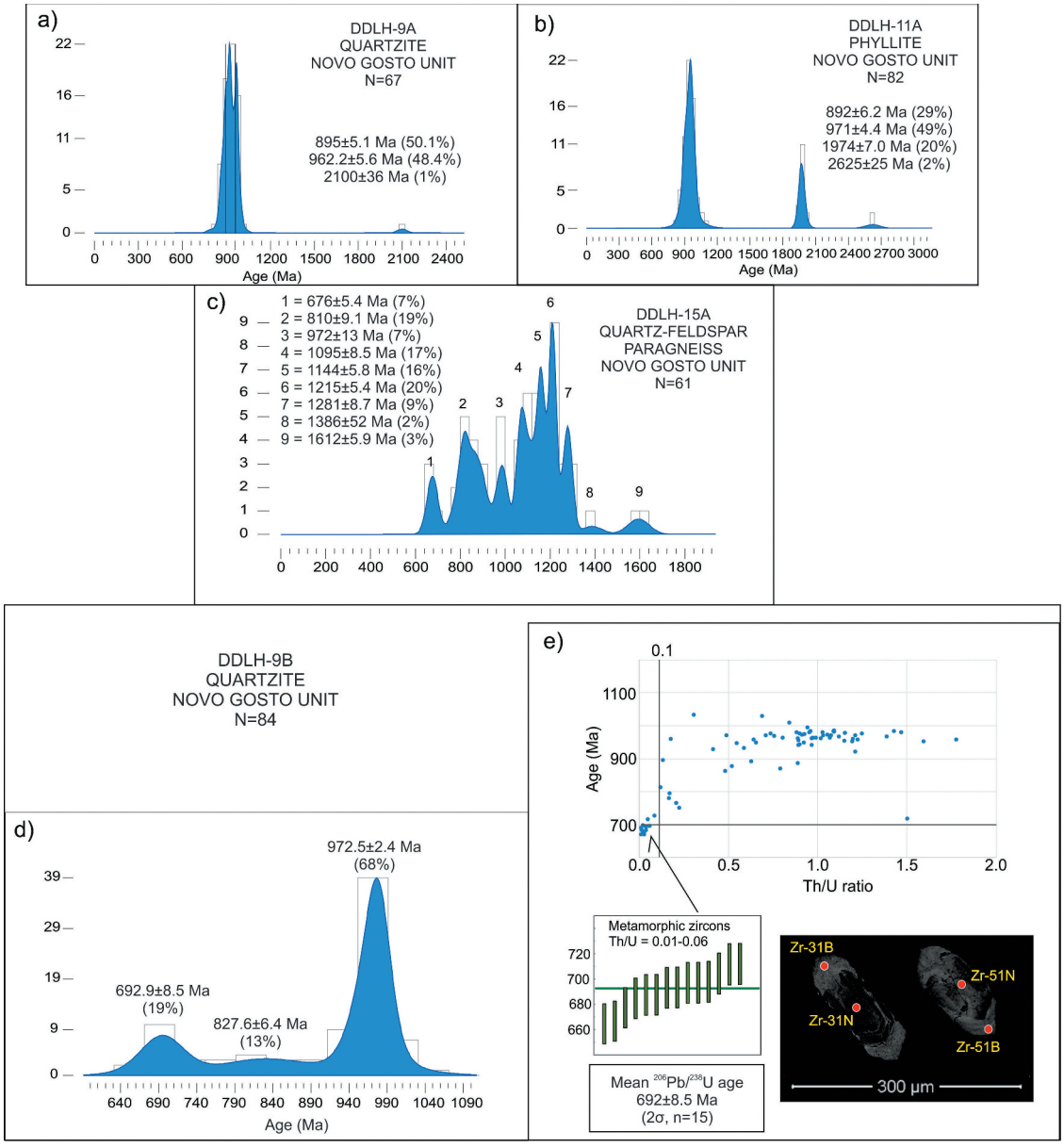

Figure 6. Frequency of occurrence of detrital zircon ages in metasedimentary samples from the Novo Gosto unit. A) Sample DDLH-9A (quartzite); B) Sample DDLH-11A (phyllite); C) Sample DMLH-15A (quartz-feldspar paragneiss); D e E) Sample DDLH-9B (quartzite).

895 ± 5.1 Ma (91%) and is interpreted as the age of the main sediment source, which is the probable maximum sedimentation age of the paleobasin.

Eighty-two zircon analyses of phyllite sample DDLH-11A resulted in four peaks of detrital zircon grains at 892 ± 6.2 Ma (29%), 971 ± 4.4 Ma (49%), 1974 ± 7 Ma (20%), and 2624 ± 25 Ma (2.5%) (Figure 6B). The main peak is well established at 971 ± 4.4 Ma and is related to the main source of sediments, while the minor peak of 892 ± 6.2 Ma is the probable maximum sedimentation age of the paleobasin.

Fifty-eight zircon analyses of quartz-feldspar paragneiss sample DMLH-15A resulted in multiple peaks of detrital zircon ages at 676.5 ± 5.4 Ma, 810 ± 9.1 Ma, 920 ± 8 Ma, 1095 ± 8.5 Ma, 1144 ± 5.8 Ma, 1215 ± 5.4 Ma, 1284 ± 8.7 Ma, 1386 ± 52 and

1612 ± 9 Ma (Figure 6C). Around 77 % of the data fall between Tonian and Steanian ages. The maximum depositional age is calculated using two youngest detrital igneous zircon grains 676.5 ± 5.4 Ma.

Eighty-four zircon analyses in quartzite sample DDLH-9B resulted in one peak of metamorphic and two peaks of detrital zircon grains at 692.6 ± 8.5 Ma (19%), 827.6 ± 6.4 Ma (13%), and 972.5 ± 2.4 Ma (68%) (Figure 6D). The main peak is well established at 972.5 ± 2.4 Ma (69%) and is interpreted as the main sediment source. The two youngest zircon grains yield an $^{206}Pb/^{238}U$ age of 763 ± 12 Ma, which is interpreted the maximum depositional age. In contrast, the younger zircon age population (692.6 ± 8.5 Ma, n = 15) has a particular characteristic, with low Th/U ratios (between 0.01 and 0.06) (Figure 6E), which we interpret as the metamorphic age of the studied metasedimentary rock of the Novo Gosto unit.

4.3.2 Canindé domain intrusive rocks

a) Canindé layered gabbroic intrusion

Three samples of the Canindé layered gabbroic intrusion were dated: DMLH-2, DMLH-3, and DMLH-6 (Supp. Material 1). All the 14 highly concordant U-Pb data obtained for sample DMLH-6 (metadolerite), were used for the construction of the Concordia diagram, resulting in an upper intercept age of 717.9 ± 23.2 Ma (2 sigma, MSWD:0.3, Figure 7A). From the 23 analyses obtained in sample DMLH-2 (dolerite), 20 highly concordant U-Pb data were used for the construction of the Concordia diagram, resulting in a Concordia age of 716.03 ± 2.65 Ma (2 sigma, MSWD:1.9, Figure 7B). The three excluded data fall out of the statistical population and/or have extremely high errors (~71 Ma). All the 38 highly concordant U-Pb data obtained for sample DMLH-3 (gabbro) were used for the construction of the Concordia diagram, resulting in a Concordia age of 719.30 ± 2.25 Ma (2 sigma, MSWD:1.1, Figure 7C).

b) Garrote metasyenogranite

The sample of mylonitized syenogranite (DMLH-13A), mapped as part of the Garrote metagranite, was collected in an outcrop showing mingling features with a fine-grained amphibolite. Twenty-eight U-Pb zircon data were obtained for this sample (Supp. Material 1), however, a large dispersion of ages were found, mostly between 750 and 512 Ma. Three older values (~800–1000 Ma) are here interpreted as xenocrysts from the basement, while a group of ages between 512 and 640 show discordance higher than 10%, thus being discarded from the final interpretation. Highly concordant values (±10%) fall between 750 and 640 Ma, although these data still have high errors (~20 Ma). Therefore, we are using for this sample the upper intercept with the Concordia diagram, which resulted in an upper intercept age of 720.3 ± 29.1 Ma (MSWD: 0.13, Figure 7D).

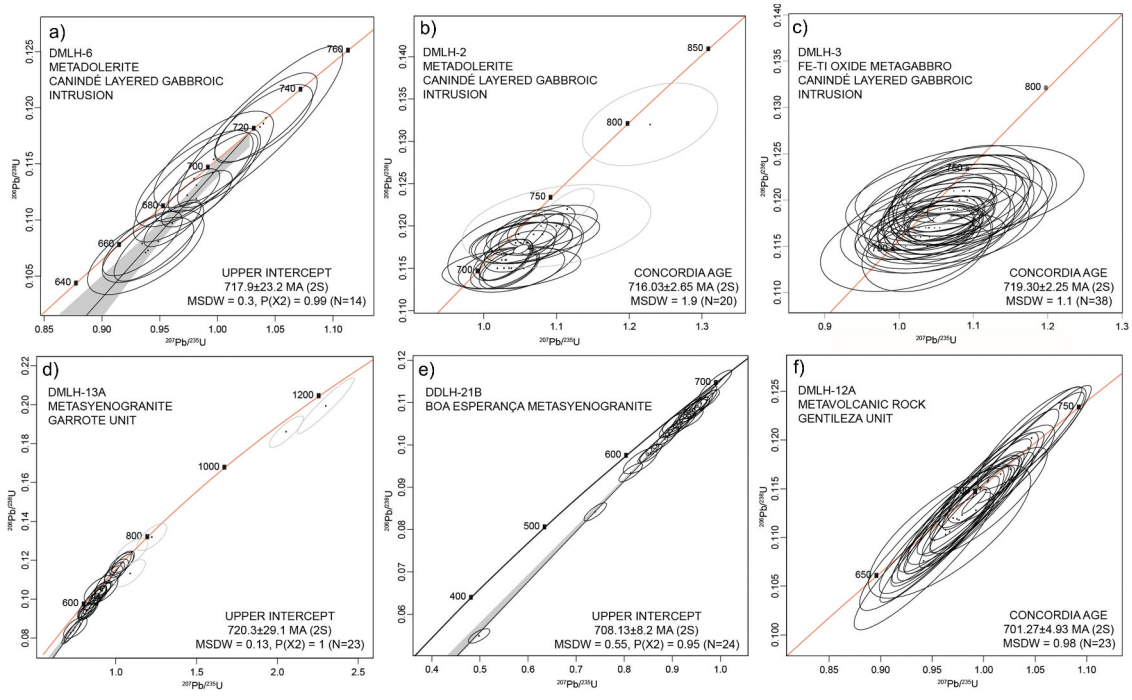

Figure 7. Diagrams with U-Pb ages of Canindé domain intrusive rocks. A) Sample DMLH-6 (metadolerite); B) Sample DMLH-2 (metadolerite); C) Sample DMLH3 (Fe-Ti oxide metagabbro); D) Sample DMLH-13A (metasyenogranite); E) Sample DDLH-21B (metasyenogranite); F) Sample DMLH-12A (metavolcanic rock).

c) Curralinho/Boa Esperança metagranite

From the Curralinho/Boa Esperança metagranite, we collected a metasyenogranite sample (DDLH-21B) with mingling features with fine-grained amphibolite. Twenty-four U-Pb ages were obtained for this sample (Supp. Material 1) and the data reveal a group of ages between 645 and 345, discordance higher than 10%. Highly concordant values (±10%) fall between 697 and 645 Ma, although with high errors (~35 Ma). Therefore, we are using for this sample the upper intercept with the Concordia diagram, which resulted in an upper intercept age of 708.13 ± 8.2 Ma (2 sigma, MSWD: 0.55, Figure 7E).

d) Gentileza metavolcanic rock

A mafic metavolcanic rock sample (DMLH-12A) of the Gentileza unit, collected in the southern portion of the Canindé domain and intrusive in rocks from the Novo Gosto unit was analyzed. Twenty-five concordant U-Pb ages were obtained for this sample (Supp. Material 1), resulting in main ages between 732 and 659 Ma. Two early Tonian ages were interpreted as xenocrysts from the basement. Twenty-three data were plotted in the Concordia diagram, resulting in a Concordia age of 701.27 ± 4.93 Ma (2 sigma, MSWD: 0.98, Figure 7F).

4.3.3 Basement rocks of the canindé domain

n the Canindé domain, we recognized tectonic slices of basement rocks represented by the samples DDLH-10A, DDLH-10B, and DMLH-12B (Supp. Material 1). The amphibolite sample DDLH-10A is from an outcrop in tectonic contact with fine-grained mylonitic granite (sample DDLH-10B). Eight highly concordant U-Pb zircon ages were obtained for this amphibolite, resulting in a Concordia age of 1005.68 ± 3.75 Ma (2 sigma, MSWD: 0.29, Figure 8A). From the mylonitic granite sample, fifty-eight zircon ages were obtained, resulting in scattering between 1072 and 816 Ma. A group of younger ages shows discordant values higher than 10%. The upper intercept of the Concordia diagram resulted in an age of 989.68 ± 6.36 Ma (2 sigma, MSWD: 1.2, Figure 8B). The sample DMLH-12B is also a fine-grained mylonitic granite and 48 zircon ages were obtained in this sample, resulting in ages between 799 and 978 Ma. All the data were plotted in the Concordia diagram, resulting in an age of 988.58 ± 16.13 Ma (2 sigma, MSWD: 0.91, Figure 8C). This latter sample occurs in an outcrop encompassed by a mafic metavolcanic rock from the Gentileza unit (sample DDLH-12A, see section referring to the Gentileza unit) in the Mulungu-Alto Bonito shear zone.

4.3.4 Poço redondo domain

To compare ages and possible sources of metasedimentary rocks from the Novo Gosto unit, we collected two samples in the neighbouring domain, the Poço Redondo domain (samples DMLH-1A and DMLH-1B) (Supp. Material 1). In the orthogneiss sample DMLH-1B (PR-1B, Figure 9A), we obtained five highly concordant data, which were plotted on the Concordia diagram, resulting in an age of 956.72 ± 12.08 Ma (2 sigma, MSWD:0.81). The DMLH-1A (PR-1A) sample is from granite that intrudes the Poço Redondo gneiss. Thirty-four U-Pb ages were obtained (Supp. Material 1), however, a large dispersion of ages between 1017 and 569 Ma was found. The group of older ages (~766–1017 Ma) is here interpreted as xenocrysts from the Poço Redondo basement, resulting in a Concordia age of 989.52 ± 7.4 (n = 7) (Figure 9B). A statistical population (10 spots), with highly concordant values (±10%), falls between 670 and 626 Ma and are possibly the zircon ages related to the granite crystallization. Concordia age of this group resulted in an age of 636 ± 3.76 Ma (Figure 9B). Two

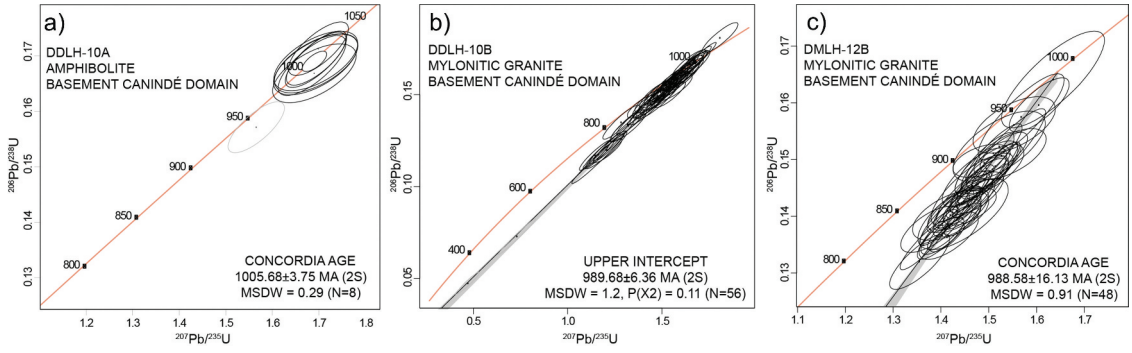

Figure 8. Diagrams with U-Pb ages of basement rocks of the Canindé domain. A) Sample DDLH-10A (amphibolite); B) Sample DDLH-10B (mylonitic granite); C) Sample DMLH-12B (mylonitic granite).

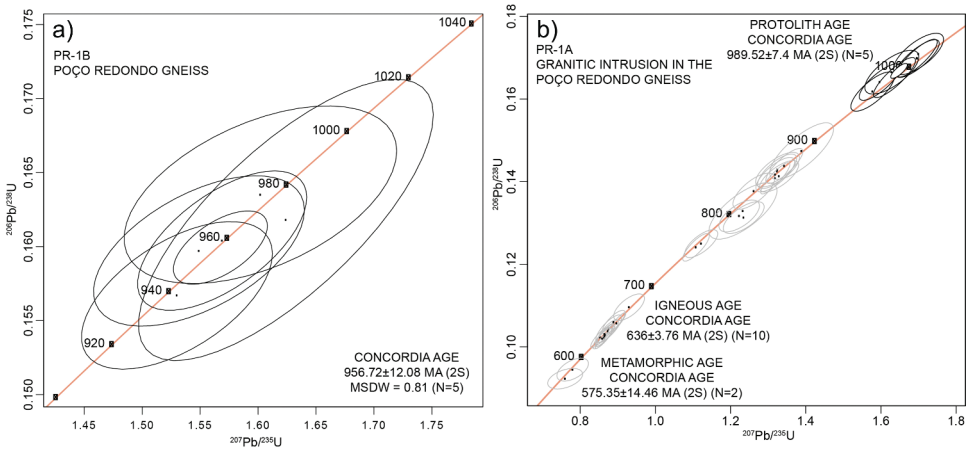

Figure 9. Diagrams with U-Pb ages of Poço Redondo domain rocks. A) Sample PR-1B (orthogneiss); B) Sample PR-1A (granite).

younger ages of 569–582 Ma are here interpreted as recrystallized zircon grains, associated with a re-heating event (metamorphism?).

4.4 Nd isotopic geochemistry

Whole-rock Sm-Nd isotopes of metasedimentary rocks from the Novo Gosto unit bring important information on the nature of the Novo Gosto basin (Supp. Table 6). Among the analyzed rock samples, there are metasandstones, metapelites, phyllites, meta-arkose, and impure metacarbonate. The ratio values of $^{147}Sm/^{144}Nd$ and $^{143}Nd/^{144}Nd$ range from 0.1047 to 0.1553 and 0.511666 to 0.512605, respectively. The values of $\varepsilon_{Nd\ (0)}$ range from −18.96 to −0.64 and the T_{DM} ages (single-stage) vary from 1.27 to 2.21 Ga. The values of $\varepsilon_{Nd\ (740\ or\ calculated\ age)}$ range from −11.25 to 3.28 and the T_{DM} ages (double-stage) range from 1.10 to 2.24 Ga (Figure 10A,B). Five samples, mica schist (CRN-210a), metasandstone (DDLH-6B), metasandstone (DDLH-1), metacarbonate (DDLH-14), metapelite (CRN-143a), have model ages close to 1.3 Ga. Other rocks, meta-arkose, metapelites, phyllite, and metasandstones show T_{DM} ages between 1.3 and 1.8 Ga. The third group of rocks (metasandstones and mica schist) displays T_{DM} ages in 2.2 Ga.

5. Discussion

5.1 Basement of the novo gosto unit

The observed field relationships in association with the obtained ages in this research resulted in the identification of rocks that represent basement fragments in the Canindé domain (samples DDLH-10A, 10B, and DMLH-12B, see section 5.3.3). The studied rocks show ages compatible with crystallization during the Cariris Velho event (early Tonian), which in the region are recognized mainly in the Poço Redondo-Marancó domain, to the south (crystallization ages between 1000 and 920 Ma, e.g. Carvalho 2005; Oliveira *et al.* 2010; Caxito *et al.* 2020) and other occurrences to the north of the area (e.g. Brito Neves *et al.*

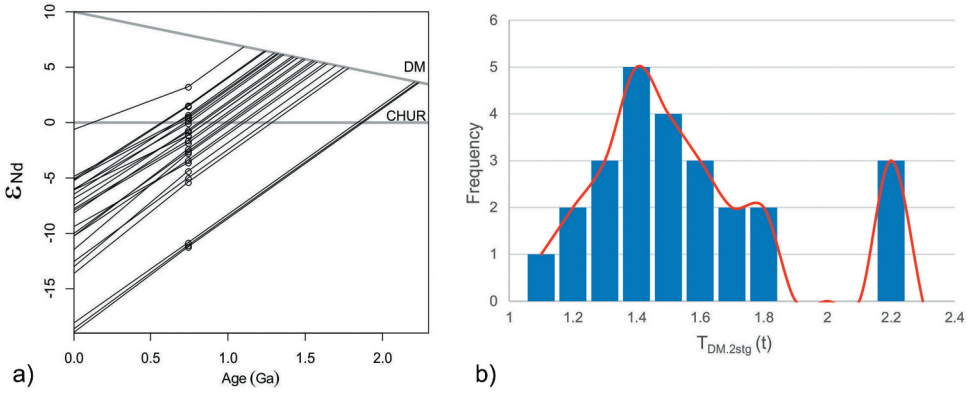

Figure 10. A) ε_{Nd} vs. Age diagram showing Nd isotope evolution for metasedimentary rocks from the Novo Gosto unit. B) Histogram of frequency of $T_{DM\text{-}2stg}$ ages of the metasedimentary rocks.

1995; Brito *et al*. 2008; Brito and Freitas 2011; Cruz and Acciolly 2013; Cruz *et al*. 2014; Silva Filho *et al*. 2014; Guimarães *et al*. 2016; Dáttoli 2017; Caxito *et al*. 2020). The samples DDLH-10A and DDLH-10B were collected in the vicinity of the limit with the Poço Redondo domain and the Mulungu-Alto Bonito shear zone, suggesting that these are fragments from the Poço Redondo domain juxtaposed to the Canindé domain units during the collision phase. The mylonitic granite (DMLH-12B) of upper intercept age 988.58 ± 16.13 Ma is intruded by the mafic volcanism of the Gentileza unit (DMLH-12A), which was dated at Concordia age of 701.27 ± 4.93 Ma. Based on the presence of these basement slices, we suggest that the basement of the Novo Gosto unit consists of the same material, which is supported by the new U-Pb detrital zircon ages and Nd model ages.

5.2 Main source area and maximum depositional age

U-Pb ages on detrital zircon grains of the three metasedimentary rocks show a main peak between 962 and 981 Ma, all of them with a high frequency of occurrence (>73%), representing a highly probable source area for the Novo Gosto paleobasin. Besides these source areas, the same samples show a Paleoproterozoic and Neoarchean source area (1974, 2624 Ma), although with a lower frequency (1–20%). One sample shows a higher range of the main peaks, between 800 and 1200 Ma (77%), being these ages rare in the adjacent areas.

The probable early Tonian source area is well known in the region, occurring even as a rare basement in the Canindé domain, as well as in the adjacent Poço Redondo-Marancó domain and other surrounding areas in the Pernambuco-Alagoas superterrane and Southern Borborema Province (e.g. Brito Neves *et al*. 1995; Brito *et al*. 2008; Brito and Freitas 2011; Cruz and Acciolly 2013; Cruz *et al*. 2014; Silva Filho *et al*. 2014; Guimarães *et al*. 2016; Dáttoli 2017; Caxito *et al*. 2020). Adjacent areas with Paleoproterozoic and Neoarchean rocks occur mostly in restricted areas, like the Jirau do Ponciano, Nicolau-Campo Grande, Belém do São Francisco complexes and minor granitic occurrences (Sá *et al*. 1995; Van Schmus *et al*. 1995; Accioly *et al*. 2000; Sá *et al*. 2002; Silva Filho *et al*. 2002; Santos *et al*. 2008b; Hollanda *et al*. 2011; Santos *et al*. 2015; Oliveira *et al*. 2015; Caxito *et al*. 2020).

The same source area groups were identified with Nd isotopes, with a positive $\varepsilon_{Nd\ (t:740)}$ and $T_{DM\ 2stage}$ between 1.10 and 1.35 and a highly negative $\varepsilon_{Nd\ (t:740)}$ and $T_{DM\ 2stage}$ of 2.2 Ga. Several samples show values in between these two groups, which can be an effect of sedimentary mixture between the two sources. Oliveira *et al*. (2015) suggested that the T_{DM} ages from the Canindé domain (1.0 to 1.6 Ga) were mostly younger than the Marancó domain ages (1.2 to 2.2 Ga), the latter domain being mostly provided by older sources. However, with the new data here obtained, we identified this older source in the Canindé domain as well, being the two domains provided by similar source areas.

The youngest zircon age obtained for the Novo Gosto metasedimentary rocks, commonly interpreted as the maximum depositional age of the paleobasin, is here defined as 676 ± 5.4 Ma (four youngest zircon grains of sample DDLH-15A). This sample may represent younger sedimentation of the Novo Gosto unit. Other samples contain older maximum depositional age of 780 ± 6.1, 892 ± 6.2, and 895 ± 5.1 Ma. The youngest age zircon population at 692.6 ± 8.5 Ma (2s, n = 15) with Th/U ratios from 0.06 to 0.01, determined in sample DMLH-9B, is interpreted here as metamorphic age, imprinted on the detrital zircon grains. Oliveira *et al*. (2015) obtained maximum depositional age for the Novo Gosto unit (metagraywacke) of approximately 650 Ma with two significant peaks at ca. 714 Ma and 995 Ma. These authors also found one zircon grain with an age of 625 Ma, interpreted as a metamorphic zircon.

These maximum depositional ages may reflect a long period of active sedimentation (~170 Ma) or most likely to be influenced by different source areas in the paleobasin. Nascimento (2005) determined approximately the depositional age of carbonate rocks from the Novo Gosto unit at 963 ± 20 Ma, which can suggest, together with the new data, long-term sedimentation for the Novo Gosto paleobasin.

Regarding the source area, we suggest that the source area of the Marancó-Poço Redondo and Canindé domains, in addition to some points of the Macururé domain, have a dominance of an early Tonian source, while in the rest of the Macururé, Vaza-Barris and Estância domains Paleoproterozoic sources dominate, implying a probable source area from the São Francisco Craton (Oliveira *et al*. 2015; Neves *et al*. 2016).

5.3 Tectono-metamorphic evolution of the novo gosto unit

Petrographic and geothermobarometric data of amphibolites from the Novo Gosto unit demonstrate that the unit was affected by clockwise P-T metamorphic conditions. The metamorphic peak occurred at the Cryogenian age, reaching the sillimanite stability field

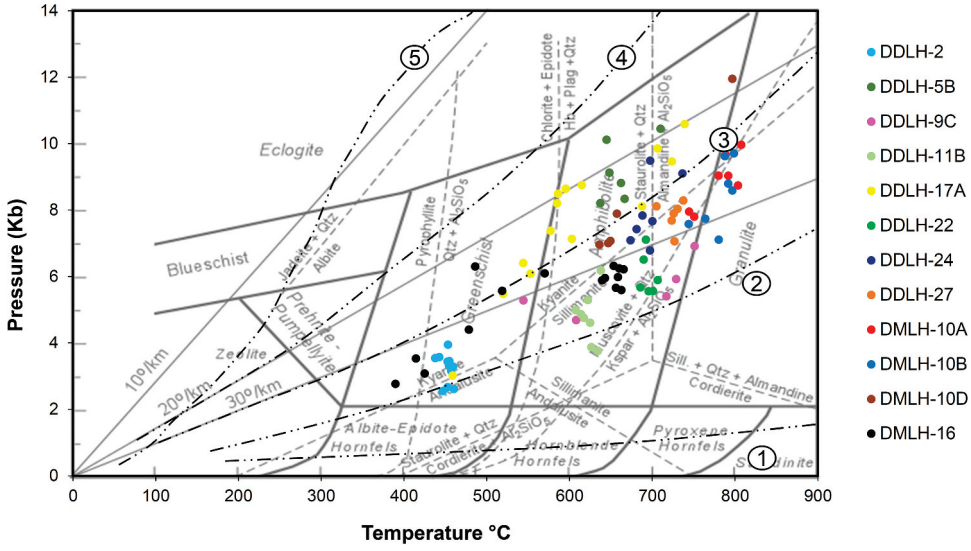

Figure 11. Amphibolite samples from the Novo Gosto Unit are plotted on the metamorphic facies diagram (P-T). (1) Contact (thermal) metamorphism, (2) Volcanic arc, (3) Collisional mountain belt, (4) Stable continent, (5) Accretionary prism (Redrawn from nelson 2004; Marshak 2019).

upper amphibolite facies conditions. Some data evidenced retrometamorphic P-T conditions in greenschist facies (Figure 11). The pressure conditions reached a maximum of 12.0 kbar and the temperature conditions of 808°C and a minimum of 2.5 kbar and 390°C. These T and P variations are most probably associated with the tectonic evolution of the metamorphic terrane, the higher P-T values associated with progressive metamorphism until it reached the metamorphic peak, while the lower P-T conditions are related to the retrogressive metamorphic path, until the complete exposure of the terrane.

The mylonitic amphibolites show the highest P and T conditions (7.0–12.0 kbars and 636–808°C). It is consistent with the textures identified in the microscale. The samples that were not mylonitized were crystallized under P and T conditions at least lower than those mylonitic rocks, ranging mainly around 600–740°C and 3.5–10.0 kbars. The calculated P-T conditions, plotted in Figure 11 have a distribution compatible with volcanic arc (path 2) evolving to a collisional mountain belt path (3).

The age of the progressive metamorphic event was obtained in sample DDLH-9B (Novo Gosto unit/quartzite), in which a group of zircon grains with very low Th/U ratios (0.01 to 0.06) was found, which are classically associated with metamorphic crystallization. Alternatively, source area zircons that were metamorphic, and then eroded and delivered to the basin. We do not discard the possibility that this age might register an uncommon event in the region and further investigation is needed. This group of zircon grains provides a $^{207}Pb/^{206}Pb$ age of 692.6 ± 8.5 Ma for the metamorphic peak, during collision and amalgamation of the Sergipano Belt. Younger metamorphic ages for the area were suggested by Oliveira *et al.* (2015), who reported age of 625 Ma in a metagraywacke from the Novo Gosto Unit and interpreted it as a metamorphic zircon.

Finally, a much younger group of concordant U-Pb zircon ages is recorded in sample DMLH-1A, with ages between 582 and 569 Ma. This sample is from the neighbouring Poço Redondo domain, and the younger age can be related to the D3 deformational event of Oliveira *et al.* (2010), suggested being around 581 Ma (Ar-Ar muscovite age in the Macururé D3 foliation).

5.4 Pre-collisional magmatic intrusions

The ages found for the metavolcanic rocks in the Novo Gosto unit (~743 Ma, Passos *et al.* 2021)characterize the older post-Cariris Velhos magmatism of the Canindé domain, followed by the other magmatic units in order of age: Canindé layered gabbroic intrusion, Garrote unit, Curralinho/Boa Esperança metagranite, and Gentileza unit. New U-Pb ages obtained in the Canindé layered gabbroic intrusion are 717.9 ± 23.2 Ma, 716.03 ± 2.65 Ma, and 719.30 ± 2.25 Ma. These ages are slightly older than the ages reported by Oliveira *et al.* (2010) of 701 ± 8 Ma and Pinto *et al.* (2020) of 703 ± 1.6 Ma. The obtained age for the Garrote metasyenogranite is an upper intercept and has a large error (720.3 ± 29.1 Ma), although it is similar to the age

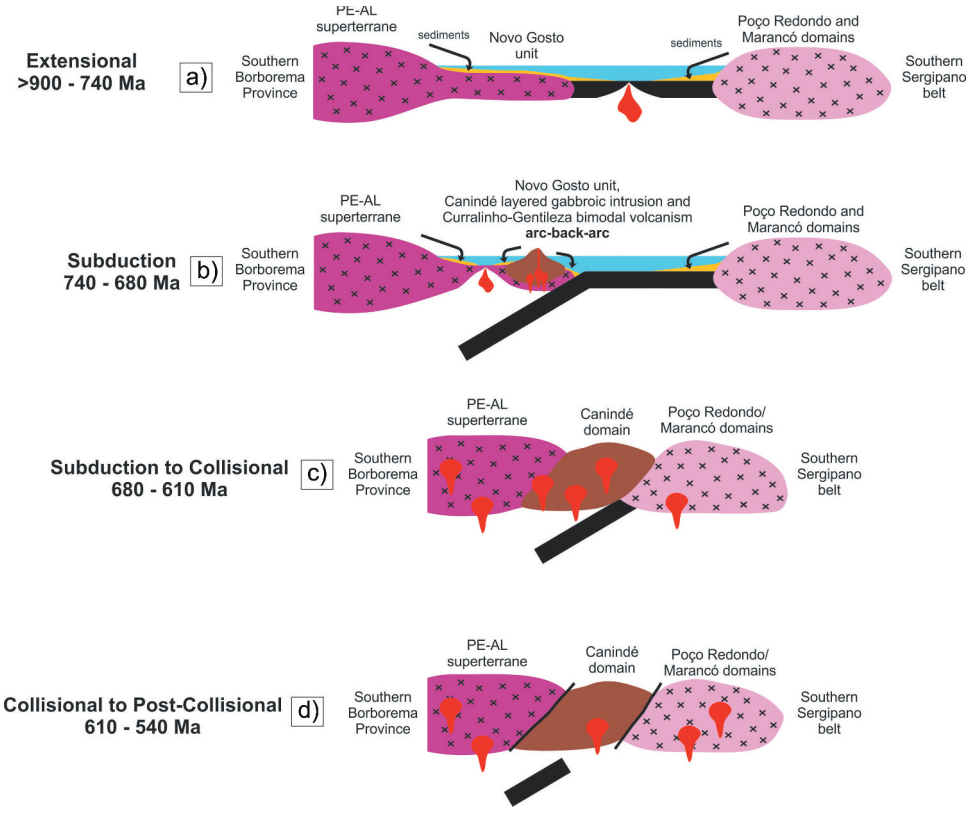

Figure 12. Proposed tectonic evolution model for the Canindé domain, Sergipano Belt. Modified after Passos *et al*. (2021).

of Van Schmus apud Santos *et al*. (1998) of 715 Ma. The Curralinho/Boa Esperança metagranite obtained an age of 708.13 ± 8.2 Ma (upper intercept) is older than the age found by Oliveira *et al*. (2010) of 641 ± 5 Ma (Boa Esperança metagranite) and 684 ± 7 (Curralinho granite). The new Gentileza metavolcanic rock age of 701.27 ± 4.93 Ma is, as well, a little older than the age of 688 ± 6 (quartz-monzodiorite) published by Oliveira *et al*. (2010).

The metavolcanic rocks of the Novo Gosto unit represent the first records of a convergence event during the early Brasiliano orogeny in the Sergipano Belt (Passos *et al*. 2021) and together with the other magmatic units mentioned are assumed as the late Tonian/Cryogenian (740–680 Ma) pre-collisional magmatism of the Sergipano Belt.

6. Conclusion

With this research, we conclude that:

(A) Late Stenian/Early Tonian crystallization ages (989.68 ± 6.36, 1005.68 ± 3.75 and 988.58 ± 16.13) were for the first time identified in amphibolite and granitic mylonites of the Canindé domain. These rocks occur near to the Mulungu-Alto Bonito shear zone, close to the contact with the Poço Redondo-Marancó domain, and possibly represent slices of this unit juxtaposed with the Canindé domain during the collisional event (Figure 12C,D).

(B) The main source area was investigated using U-Pb detrital zircon ages and Nd isotopes. The U-Pb ages in the Novo Gosto metasedimentary rocks reveal that the most probable and important source area for the Novo Gosto paleobasin has ages of 962–978 Ma. A minor Paleoproterozoic and Neoarchean source area was identified too (1974–2624 Ma). The probable Early Tonian source is well known in the adjacent Poço Redondo-Marancó domain and other areas of the Pernambuco-Alagoas superterrane and Southern Borborema Province, but also found as rare basement slivers within the Canindé domain (Figure 12A,B). In the Borborema Province, the presence of Paleoproterozoic and Neoarchean rocks is more restricted and they occur mainly in domes. Nd isotopes yielded Mesoproterozoic TDM ages in between the Paleoproterozoic/Archean ages and the Neoproterozoic igneous rocks, indicating a mixture of the two end-members and confirming that these two sources dominate.

(C) The maximum depositional age obtained for the Novo Gosto paleobasin is 676 ± 5.4 Ma, deposited after the main metamorphism of this unit. However, other samples show values of 895 ± 5.1, 892 ± 6.2 Ma, and 780.4 ± 6.1 Ma, which can reflect long-term sedimentation of the paleobasin with different source areas (Figure 12B).

(D) The tectono-metamorphic evolution of the Novo Gosto unit is here characterized as a clockwise P-T path, with metamorphic conditions ranging mainly around 600–740°C and 3.5–10.0 kbars, with peak metamorphic compatible with upper amphibolite facies. And values ranging mainly around 636–808°C and 7.0–12.0 kbars for mylonites. The minimum metamorphic conditions imprint in these rocks is T: 390°C and P: 2.5 kbar, characteristic of greenschist facies, and possibly related to the uplift of the metamorphic terrane. The path distribution of the samples is compatible with a volcanic arc evolving to a collisional mountain belt environment. Age of 692.6 ± 8.5 Ma ($^{207}Pb/^{206}Pb$ zircon age/LA-ICPMS) calculated from data obtained on zircon rims with a low Th/U ratio from a quartzite was associated with the progressive metamorphic peak (Figures 12C,D). Alternatively, those zircons could have been eroded from source areas that record this metamorphic event and incorporated in the basin

(E) Ages of 740–680 Ma pre-collisional magmatism are recorded in the Novo Gosto unit, Canindé layered gabbroic intrusion, Garrote, Gentileza and Curralinho/Boa Esperança metagranites (Figure 12B).

(F) These new results together with those of Passos *et al*. (2021) support an accretionary-collisional evolution to the Sergipano Belt, as proposed to other sectors of the Borborema Province (eg, Del-rey Silva 1995; Santos 1995; Kozuch 2003; Oliveira *et al*. 2010; Amaral *et al*. 2012; Caxito *et al*. 2014, 2020, 2021; Santos *et al*. 2014; Lima *et al*. 2015, 2017, 2018; Lages and Dantas 2016; Padilha *et al*. 2016) and contradict the intracontinental evolutionary model for the province (Neves 2003; Neves *et al*. 2006, 2015).

(G) These new data and those of Passos *et al*. (2021) provide important information about the pre-collisional phase of the Sergipano Belt, and contribute to possibilities of correlation between the South Borborema Province and the Central African Orogen.

Highlights

- Data sets a perspective for future correlations with adjacent belts
- Data for structuration of West Gondwana, in Brasiliano-Pan African Orogeny
- New U-Pb zircon ages for Sergipano Belt, Borborema Province
- Late Stenian to early Tonian basement for the Canindé domain

Acknowledgments

This study was financed in part by the Coordenação de Aperfeiçoamento de Pessoal de Nível Superior (CAPES), Brasil, Finance Code 001. Support of the CAPES fellowship (grant n° 88882.347179/2019-01) and INCT Estudos Tectônicos research grant were essential for this research and the continuity of future work. RAF and FC acknowledge CNPq research fellowships. We thank Márcio Martins Pimentel (in memoriam) for the contribution.

Disclosure statement

No potential conflict of interest was reported by the author(s).

ORCID

Reinhardt A. Fuck http://orcid.org/0000-0003-1396-125X
Lauro Cézar M. de Lira Santos http://orcid.org/0000-0001-6098-1873

References

Accioly, A.C.A., McReath, I., Santos, E.J., Guimarães, I.P., Vannuci, R., and Bottazzi, R., 2000, The passira meta-anorthositic complex and its tectonic implication, Borborema Province, Brazil. 31st international geological congress, International Union of Geological Sciences, Abstracts: Rio de Janeiro.

Aleinikoff, J. N., Wintsch, R. P., Fanning, C. and Dorais, M. J., 2002. U–Pb geochronology of zircon and polygenetic titanite from the Glastonbury Complex, Connecticut, USA: an integrated SEM, EMPA, TIMS, and SHRIMP study. Chemical Geology, 188, 1–2, 125–147. 10.1016/S0009-2541(02)00076-1

Amaral, W.S., Santos, T.J.S., Wernick, E., Nogueira Neto, J.A., Dantas, E.L., and Matteini, M., 2012, High-pressure granulites from Cariré, Borborema Province, NE Brazil: Tectonic setting, metamorphic conditions and U-Pb, Lu-Hf and Sm-Nd geochronology: Gondwana research, 22, 892–909. 10.1016/j.gr.2012.02.011.

Brito Neves, B.B., Fuck, R.A., and Pimentel, M.M., 2014, The Brasiliano collage in South America: A review: Brazilian Journal of Geology, 44, 3 493–518. 10.5327/Z2317-4889201400030010.

Brito Neves, B.B., Sial, A.N., and Albuquerque, J.P.T., 1977, Vergência centrífuga residual no Sistema de Dobramentos Sergipano: Revista Brasileira de Geociências, 7, 2 102–114. 10.25249/0375-7536.1977102114

Brito Neves, B.B., and Silva Filho, A.F., 2019, Superterreno Pernambuco-Alagoas na Província Borborema: Ensaio de regionalização tectônica: Geologia USPSérie Científica, 19, 2 3–28. 10.11606/issn.2316-9095.v19-148257.

Brito Neves, B.B., Van Schmus, W.R., and Fetter, A.H., 2001, Noroeste da África – Nordeste do Brasil (Província Borborema) Ensaio comparativo e problemas de correlação: Geologia USPSérie Científica, 1, 59–78. 10.5327/S1519-874X2001000100005 1.

Brito Neves, B.B., Van Schmus, W.R., Santos, E.J., Campos Neto, M.C., and Kozuch, M., 1995, O evento Cariris Velhos na Província Borborema: Integração de dados, implicações e perspectivas: Braz. J. Geol, 25, 279–296.

Brito, M.F.L., and Freitas, S., 2011. Caracterização petrológica e geotectônica do ortognaisse Lobo no domínio Pernambuco-Alagoas, Província Borborema; Nordeste do Brasil. In: XIII Brazilian Geochemical Congress. Gramado-RS, Brazil. Extended Abstract e CD-ROM, 796–799

Brito, M.F.L., Mendes, V.A., and Paiva, I.P., 2008. Metagranitóide Serra das Flores: Magmatismo Toniano (tipo-A) no Domínio Pernambuco-Alagoas, Nordeste do Brasil. In: 44° Brazilian Geological Congress, Curitiba. Abstract in CD-ROM.

Bühn, B., Pimentel, M.M., Matteini, M., and Dantas, E.L., 2009, High spatial resolution analysis of Pb and U isotopes for geochronology by laser ablation multicollector inductively coupled plasma mass spectrometry (LA-MC-ICP-MS): Anais da Academia Brasileira de Ciências, 81, 1 1–16. 10.1590/S0001-37652009000100011.

Carvalho, M.J.C., 2005. Evolução tectônica do Domínio Marancó-Poço Redondo, margem norte da Faixa Sergipana. Tese de Doutorado, Campinas: Instituto de Geociências, Universidade Estadual de Campinas. p.200.

Caxito, F.A., Basto, C.F., Santos, L.C.M.L., Dantas, E.L., Medeiros, V.C., Dias, T.G., Barrote, V., Hagemann, S., Alkmim, A.R., and Lana, C., 2021, Neoproterozoic magmatic arc volcanism in the Borborema Province, NE Brazil: Possible flare-ups and lulls and implications for western Gondwana assembly: Gondwana research, 92, 1–25. 10.1016/j.gr.2020.11.015

Caxito, F.A., Santos, L.C.M.L., Ganade, C.E., Bendaoud, A., Fettous, E.-H., and Bouyo, M.H., 2020, Toward an integrated model of geological evolution for NE Brazil–NW Africa: The Borborema Province and its connections to the Trans-Saharan (Benino-Nigerian and Tuareg shields) and Central African orogens: Brazilian Journal of Geology. 50, 2 1–38. https://doi.org/10.1590/2317-4889202020190122.

Caxito, F.A., Uhlein, A., and Dantas, E.L., 2014, The Afeição augen-gneiss suíte and the recorf of the Cariris Velhos Orogeny (1000-960 Ma) within the riacho do pontal fold belt: Journal of South American Earth sciences, 51, 12–27. 10.1016/j.jsames.2013.12.012

Cerny, J., Ramírez-Herrera, M.-T., Bógalo, M.F., Goguitchaichvili, A., Castillo-Aja, R., and Morales, J., 2016, Origen, hidrodinámica y variación lateral en sedimentos de tsunami por ams, Costa Mexicana Del Pacífico: Latinmag Lett, 6, 1–7.

Chemale, F., Jr., Kawashita, K., Dussin, I.A., Avila, J.N., Justino, D., and Bertotti, A.L., 2012, U-Pb zircon in situ dating with LA-MC-ICP-MS using a mixed detector configuration: Anais da Academia Brasileira de Ciências, 84, 275–295. 10.1590/S0001-37652012005000032 2.

Compston, W., Williams, I.M., and Myer, C., 1984, U-Pb geochronology of zircons from lunar breccia 73217 using a sensitive high mass-resolution ion microprobe: journal of Geophysical Research, 89B, 525–534. 10.1029/JB089iS02p0B525 S02.

Cornell, R.M., and Schwertmann, U., 2003, The Iron Oxides, Second Wiley VCH: Weinheim. 664.

Cruz, R.F., and Acciolly, A.C.A., 2013, Petrografia, geoquímica e idade U/Pb do Ortognaisse Rocinha, no Domínio Pernambuco-Alagoas W da Província Borborema: Estudios Geologicos, 23, 2 3–27.

Cruz, R.F., Pimentel, M.M., Accioly, A.C.A., and Rodrigues, J.B., 2014, Geological and isotopic characteristics of granites from the Western pernambuco-alagoas domain: Implications for the crustal evolution of the Neoproterozoic Borborema Province: Brazilian Journal of Geology, 44, 4 627–652. 10.5327/Z2317488920140004000 8.

D'el-rey Silva, L.J.H., 1995, Tectonic evolution of the sergipano belt, NE Brazil: Geologia, 25, 4 315–332.

Dáttoli, L.C., 2017. Geologia, petrologia e geoquímica do ortognaisse Maravilha, domínio Pernambuco-Alagoas. Dissertação de Mestrado. Pós-graduação em geociências, UFPE, 123p.

Davison, I., and Santos, R.S., 1989, Tectonic evolution of the sergipano belt, NE do Brasil, during the brasiliano orogeny: Precambrian research, 45, 319–342. 10.1016/0301-9268(89)90068-5 4.

Deer, W.A., Howie, R.A., and Zussman, J., 1992, An introduction to the rock forming minerals. 3rd ed. London: The Mineralogical Society, 549.

Ernst W.G., and Liu J. 1998. Experimental phase-equilibrium study of Al- and Ti-contents of calcic amphibole in MORB; a semiquantitative thermobarometer. American Mineralogist, 83, 9–10, 952–969. 10.2138/am-1998-9-1004

Gioia, S.M.C.L., and Pimentel, M.M., 2000, The Sm-Nd isotopic method in the geochronology laboratory of the university of Brasília: Anais da Academia Brasileira de Ciências, 72, 2 219–245. 10.1590/S0001-37652000000200009.

Goldstein, S.L., O'Nions, R.K., and Hamilton, P.J., 1984, A Sm-Nd isotopic study of atmospheric dusts and particulates from major river systems: Earth and Planetary Science Letters, 70, 221–236. doi:10.1016/0012- 821X(84)90007-4 2.

Guimarães, I.P., Brito, M.F.L., Lages, G.A., Silva Filho, A.F., Santos, L., and Brasilino, R.G., 2016, Tonian granitic magmatism of the Borborema Province, NE Brazil: A review: Journal of South American Earth sciences, 68, 97–112. 10.1016/j.jsames.2015.10.009

Hollanda, M.H.B.M., Archanjo, C.J., Souza, L.C., Dunyi, L., and Armstrong, R.A., 2011, Long lived paleoproterozoic granitic magmatism in the serido-jaguaribe domain, Borborema province NE Brazil: Journal of South American Earth sciences, 32, 287–300. https://doi.org10.1016/j 4. jsames.2011.02.008.

Jackson, S.E., Pearson, N.J., Griffin, W.L., and Belousova, E.A., 2004, The application of laser ablation inductively coupled plasma-mass spectrometry to in situ U-Pb zircon geochronology: chemical Geology, 211, 47–69. 10.1016/j.chemgeo.2004.06.017 1–2.

Janoušek, V., Moyen, J.-F., Erban, V., and Hora, J. 2019. GCDkit goes platform independent! Abstracts of the Goldschmidt Conference, Barcelona, Spain.

Kozuch, M., 2003. Isotopic and trace element geochemistry of Early Neoproterozoic gneissic and metavolcanic rocks in the Cariris Velhos Orogen of the Borborema Province, Brazil, and their bearing tectonic setting (PhD thesis). Kansas University, Lawrence, p. 199.

Lages, G.A., and Dantas, E.L., 2016, Floresta and bodocó mafic-ultramafic complexes, western Borborema Province, Brazil: Geochemical and isotope constraints for evolution of a neoproterozoic arc environment and retro-eclogitic hosted Ti-mineralization: Precambrian research, 280, 95–119. 10.1016/j.precamres.2016.04.017.

Leake, B.E., Woolley, A.R., Arps, C.E.S., Birch, W.D., Gilbert, M. C., Grice, J.D., Hawthorne, F.C., Kato, A., Kisch, H.J., Krivovichev, V.G., Linthout, K., Laird, J., Mandarino, J.A., Maresch, W.V., Nickel, E.H., Rock, N.M.S., Schumacher, J.C., Smith, D.C., Stephenson, N.C.N., Ungaretti, L., Whittaker, E.J.W., and Youzhi, G., 1997, Nomenclature of amphiboles: report of the subcommittee on amphiboles of the international mineralogical association: Commission on New Minerals and Mineral Names. Am. Mineral, 82, 1019–1037.

Lima, M.V.A.G., Berrocal, J., Soares, J.E.P., and Fuck, R.A., 2015, Deep seismic refraction experiment in northeast Brazil: New constraints for Borborema province evolution: Journal of South American Earth sciences, 58, 335–349. 10.1016/j.jsames.2014.10.007

Lima, H.M., Pimentel, M.M., Fuck, R.A., Santos, L.C.M.L., and Dantas, E.L., 2018, Geochemical and detrital zircon geochronological investigation of the metavolcanosedimentary araticum complex, sergipano fold belt: Implications for the evolution of the Borborema Province: Journal of South American Earth sciences, 86, 176–192. 10.1016/j.jsames.2018.06.013

Lima, H.M., Pimentel, M.M., Santos, L.C.M.L., and Mendes, V.A., 2017, Análise tectônica da porção nordeste da Faixa Sergipana, Província Borborema: Dupla vergência em resposta a colisão oblíqua entre o Cráton do São Francisco e o Terreno Pernambuco-Alagoas: Geonomos, 25, 2 20–30.

Ling, -X.-X., Schmädicke, E., Li, Q.-L., Gose, J., Wu, R.-H., Wang, S.-Q., and Li, X.-H., 2015, Age determination of nephrite by in-situ SIMS U–Pb dating syngenetic titanite: A case study of the nephrite deposit from Luanchuan, Henan, China. Lithos 220-223 289–299. 10.1016/j.lithos.2015.02.019.

Ludwig, K.R., 2003. User's manual for isoplot/Ex version 3.00 – A geochronology toolkit for microsoft excel, no. 4. Berkeley Geochronological Center, Special Publication, 70p.

Marshak, S., 2019, Earth: Portrait of a planet. 6ed, W. W. Norton & Company: New York. 1008.

Nascimento, R.S., 2005, Domínio Canindé, Faixa Sergipana, Nordeste do Brasil: Um estudo geoquímico e isotópico de uma sequência de rifte continental Neoproterozóica, Tese de Doutorado, Campinas: Instituto de Geociências, Universidade Estadual de Campinas. p.159.

Nelson, S.A., 2004, Metamorphic rocks- classification, field gradients, & facies: Lecture Note, Earth and Environmental Sciences, 2120, Petrology. Available in http://www.tulane.edu/~sanelson/eens212/metaclassification&facies.htm.

Neves, S.P., 2003, Proterozoic history of the Borborema Province (NE Brazil): Correlations with neighboring Cratons and Pan-African belts and implications for the evolution of western Gondwana: Tectonics, 22, 1031–1044. 10.1029/2001TC001352 4.

Neves, S.P., Bruguier, O., Silva, J.M.R., Mariano, G., Da Silva Filho, A.F., and Teixeira, C.M.L., 2015, From extension to shortening: Dating the onset of the Brasiliano orogeny in eastern Borborema Province (NE Brazil): Journal of South American Earth sciences, 58, 238–256. 10.1016/j.jsames.2014.06.004

Neves, S.P., Bruguier, O., Vauchez, A., Bosch, D., Silva, J.M.R., and Mariano, G., 2006, Timing of crustal formation, deposition of supracrustal sequences and transamazonian and Brasiliano metamorphism in eastern Borborema Province (NE Brazil): Implications for western Gondwana assembly: Precambrian research, 149, 197–216. 10.1016/j.precamres.2006.06.005 3–4.

Neves, S.P., Silva, J.M.R., and Bruguier, O., 2016, The transition zone between the pernambuco-alagoas domain and the Sergipano Belt (Borborema Province, NE Brazil) : Geochronological constraints on the ages of deposition, tectonic setting and metamorphism of metasedimentary rocks: Journal of South American Earth sciences, 72, 266–278. 10.1016/j.jsames.2016.09.010

Oliveira, E.P., McNaughton, N.J., Windley, B.F., Carvalho, M.J., and Nascimento, R.S., 2015, Detrital zircon U–Pb geochronology and whole-rock Nd-isotope constraints on sediment provenance in the neoproterozoic sergipano orogen, Brazil: From early passive margins to late foreland basins: Tectonophysics, 662, 183–194. 10.1016/j.tecto.2015.02.017

Oliveira, E.P., Windley, B.F., and Araújo, M.N.C., 2010, The neoproterozoic sergipano orogenic belt, NE Brazil: A complete plate tectonic cycle in western Gondwana: Precambrian research, 181, 64–84. 10.1016/j.precamres.2010.05.014 1–4.

Padilha, A.L., Vitorello, Í., Pádua, M.B., and Marcelo., Fuck, R.A., 2016, Deep magnetotelluric signatures of the early neoproterozoic cariris velhos tectonic event within the transversal sub-province of the Borborema Province: NE Brazil. Precambrian Res, 275, 7–83. 10.1016/j.precamres.2015.12.012

Passos, L.H., Fuck, R.A., Chemale, F., Jr., Lenz, C., Pimentel, M.M., Machado, A., and Pinto, V.M., 2021, Neoproterozoic (740-690 Ma) Arc-Back-Arc magmatism in the sergipano belt, Southern Borborema, Brazil: Journal of South American Earth sciences, 109, 103280. 10.1016/j.jsames.2021.103280

Pinto, V.M., Koester, E., Debruyne, D., Chemale, F., Jr., Marques, J.C., Passos, L.H., and Lenz, C., 2020, Petrogenesis of the mafic-ultramafic Canindé layered intrusion, Sergipano Belt, Brazil: Constraints on the metallogenesis of the associated Fe–Ti oxide ores: Ore Geology Reviews, 122. 10.1016/j.oregeorev.2020.103535.

Piper, J.D.A., 1987, Paleomagnetism and the continental crust, Wiley: New York – Toronto. 434.

Rasmussen, B., Fletcher, I.R., and Muhling, J.R., 2013, Dating deposition and low-grade metamorphism by in situ U/Pb geochronology of titanite in the paleoproterozoic timeball hill formation, Southern Africa: chemical Geology, 351, 29–39. 10.1016/j.chemgeo.2013.04.015.

Sá, J.M., Bertrand, J.M., Leterrier, J., and Macedo, M.H.F., 2002, Geochemistry and geochronology of pre-Brasiliano rocks from the transversal zone, Borborema Province,

Northeast Brazil: Journal of South American Earth Sciences, 14, 851–866. https://doi.org10.1016/S0895-9811(01)00081-5 8.

Sá, J.M., McReath, I., and Leterrier, J., 1995, Petrology, geochemistry and tectonic setting of proterozoic igneous suites of the orós fold belt (Borborema Province, Northeast Brazil): Journal of South American Earth sciences, 8, 299–314. https://doi.org/10.1016/0895-9811(95)00015-8 3–4.

Santos, E.J., 1995. O complexo granítico Lagoa das Pedras: acresção e colisão na região de Floresta (Pernambuco), Província Borborema (PhD thesis). Instituto de Geociências da Universidade de São Paulo, São Paulo, p. 228.

Santos, L.C.M.L., and Caxito, F.A., 2021, Accretionary models for the neoproterozoic evolution of the Borborema Province: Advances and open questions: Brazilian Journal of Geology, 51, 2 10.1590/2317-4889202120200104.

Santos, L.C.M.L., Dantas, E.L., Santos, E.J., Santos, R.V., and Lima, H.M., 2015, Early to late paleoproterozoic magmatism in NE Brazil: The alto moxoto terrane and its tectonic implications for the pre-Western Gondwana assembly: Journal of South American Earth sciences, 58, 188–209. https://doi.org/10.1016/j.jsames.2014.07.006.

Santos, T.J.S., Fetter, A.H., and Nogueira Neto, J.A., 2008, Comparisons between the northwestern Borborema Province, NE Brazil, and the southwestern pharusian-Dahomey belt, SW Central Africa: geological Society, London, Special Publications, 294, 101–119. h ttps://doi.org10.1144/SP294.6 1.

Santos, L.C.M.L., Lages, G.A., Caxito, F.A., Dantas, E.L., Cawood, P.A., Lima, H.M., and Lima, F.J.C., 2021, Isotopic and geochemical constraints for a paleoproterozoic accretionary orogen in the Borborema Province, NE Brazil: Implications for reconstructing Nuna/Columbia: Geoscience Frontiers, 10.1016/j.gsf.2021.101167.

Santos, M.M., Lana, C., Scholz, R., Buick, I., Schmitz, M.D., Kamo, S.L., Gerdes, A., Corfu, F., Tapster, S., Lancaster, P., Storey, C.D., Basei, M.A.S., Tohver, E., Alkmim, A., Nalini, H., Krambrock, K., Fantini, C., and Wiedenbeck, M., 2017, A new appraisal of Sri Lankan BB zircon as a reference material for LA-ICP-MS U-Pb geochronology and Lu-Hf isotope tracing: Geostandards and Geoanalytical research, 41, 3 335–358. 10.1111/ggr.12167

Santos, R.A., Martins, A.A.M., and Neves, J.P., 1998, Geologia e recursos minerais do estado de Sergipe. Aracaju: CPRM/Codise. p.107.

Santos, A.C.L., Padilha, A.L., Fuck, R.A., Pires, A.C.B., Vitorello, I., and Pádua, M.B., 2014, Deep structure of a stretched lithosphere: Magnetotelluric imaging of the southeastern Borborema province: NE Brazil. Tectonophysics, 610, 39–50. 10.1016/j.tecto.2013.10.008

Silva Filho, M.A., 1998. Arco vulcânico Canindé-Marancó e a Faixa Sul-Alagoana: sequências orogênicas Mesoproterozóicas. XLCongresso Brasileiro de Geologia, Belo Horizonte: Anais do XL Congresso Brasileiro de Geologia. p.16.

Silva Filho, A.F., Guimarães, I.P., and Van Schmus, W.R., 2002, Crustal evolution of the pernambuco-alagoas complex, Borborema Province, NE Brazil: Nd isotopic data from neoproterozoic granitoids: Gondwana research, 5, 2 409–422. 10.1016/S1342-937X(05)70732-2.

Silva Filho, A.F., Guimarães, I.P., Van Schmus, W.R., Armstrong, R.A., Santos, L.S., Concentino, L.M., and Lima, D., 2014. Shrimp oxygen, U-Pb, and Hf data of tonian orthogneiss, evidence of juvenile crust in the pernambuco e alagoas domain of the Borborema Province, NE Brazil. In: 9th South American Symposium on Isotope Geology (São Paulo: Program and Abstracts), p.95.

Sláma, J., Kosler, J., Condon, D.J., Crowley, J.L., Gerdes, A., Hanchar, J.M., Horstwood, M.S.A., Morris, G.A., Nasdala, L., Norberg, N., Schaltegger, U., Schoene, B., Tubrett, M.N., and Whitehouse, M.J., 2008, Plesovice zircon - a new natural reference material for U-Pb and Hf isotopic microanalysis: chemical Geology. 249, 1–2 1-35. https://doi:10.1016/j.chemgeo.2007.11.005.

Stacey, J.S., and Kramer, J.D., 1975, Approximation of terrestrial lead isotope evolution by a two-stage model: Earth and Planetary Science Letters, 26, 207–221. 10.1016/0012-821X(75)90088-6 2.

Van Achterbergh, E., Ryan, C.G., Jackson, S.E., and Griffin, W. L., 2001, Data reduction software for LA-ICP-MS: Appendix, Sylvester, P.J. ed. Laser ablation-ICP-mass spectrometry in the earth sciences: Principles and applications, MAC short courses series 29, Ottawa: Mineralogical Association of Canada. 239–243.

Van Schmus, W.R., Brito Neves, B.B., Hackspacher, P.C., and Babinski, M., 1995, U/Pb and Sm/Nd geochronologic studies of Eastern Borborema Province, northeastern Brazil: Initial conclusions: Journal of South American Earth sciences, 8, 267–288. https://doi:10.1016/0895-9811(95)00013-6 3–4.

Vermeesch, P., 2018, IsoplotR: A free and open toolbox for geochronology: geoscience Frontiers, 9, 1479–1493. 10.1016/j.gsf.2018.04.001 5.

Wiedenbeck M., Allé P., Corfu F., Griffin W., Meier M., Oberli F., Quadt A. Von, Roddick J. and SPIEGEL W., 1995. Three natural zircon standards for U-Th-Pb, Lu-Hf, trace element and REE analyses. Geostandards and Geoanalytical Research, 19, 1, 1–23. 10.1111/j.1751-908X.1995.tb00147.x

Wiedenbeck, M., Hanchar, J.M., Peck, W.H., Sylvester, P., Valley, J., Whitehouse, M., Kronz, A., Morishita, Y., Nasdala, L., Fiebig, J., Franchi, I., Girard, J.-P, Greenwood, R.C., Hinton, R., Kita, N., Mason, P.R.D., Norman, M., Ogasawara, M., Piccoli, P.M., Rhede, D., Satoh, H. *et al* ., 2004. Further Characterisation of the 91500 Zircon Crystal. Geostand Geoanalyt Res, 28, 1, 9–39. 10.1111/j.1751-908X.2004.tb01041.x

Williams, I.S., 1998, U-Th-Pb geochronology by ion microprobe. McKibben, M.A., Shanks, I.I.I.W.C., and Rydley, W.I. eds. Applications of microanalytical techniques to understanding mineralizing processes, Littleton: Reviews in Econ. Geol, Vol. 7. 1–35.

Yavuz, F., and Döner, Z., 2017, WinAmptb: A windows program for calcic amphibole thermobarometry: Period. Mineral, 86, 135–167. 10.2451/2017PM710

Yavuz, F., Kumral, M., Karakaya, N., Karakaya, M.Ç., and Yildirim, D.K., 2015, A windows program for chlorite calculation and classification: computers & Geosciences, 81, 101–113. 10.1016/j.cageo.2015.04.011

Zane, A., and Weiss, Z., 1998, A procedure for classifying rock-forming chlorites based on microprobe data: Rendiconti Lincei Sci. Fis. Nat. Ser, 9, 1 51–56. 10.1007/BF02904455.